Dispersed ground ice of permafrost peatlands: Potential unaccounted carbon, nutrient and metal sources

Artem Lim, Sergey Loiko, Daria Kuzmina, Ivan Krickov, Liudmila Shirokova, Sergey Kulizhsky, Sergey Vorobyev, Oleg Pokrovsky

Dispersed Ground Ice of Permafrost Peatlands:

Potential Unaccounted Carbon, Nutrient and Metal Sources

Artem G. Lim[1], Sergey V. Loiko[1,2], Daria M. Kuzmina[1], Ivan V. Krickov[1], Liudmila S. Shirokova[3,4] , Sergey P. Kulizhsky[1], Sergey N. Vorobyev[1], Oleg S. Pokrovsky[3*]

[1] BIO-GEO-CLIM Laboratory, Tomsk State University, Lenina av., 36, Tomsk, Russia
[2] Tomsk Oil and Gas Research and Design Institute (TomskNIPIneft), Prospect Mira 72, Tomsk, Russia
[3] Geoscience and Environment Toulouse (GET), UMR 5563 CNRS University of Toulouse, 14 Avenue Edouard Belin, 31400 Toulouse, France,
[4] Institute of Ecological Problem of the North, 23 Nab Severnoi Dviny, Arkhangelsk, Russia

*oleg.pokrovsky@get.omp.eu

Keywords: peat, porewater, ice, carbon, trace element, permafrost, thaw, western Siberia

Synopsis: Dispersed ground ice in permafrost peatlands contains sizable amounts of labile C and metals that can be quickly mobilized in aquatic systems upon permafrost thaw; this may strongly increase riverine export of carbon, phosphorus and some metals.

Highlights :

- Dispersed ground ice in permafrost peatlands contains sizable amount of labile C, metal and nutrients;
- We discovered a local maximum of strong enrichment in DOC, P, Ca, Mg, Mn, Fe, Sr, As 30-50 cm below the active layer;
- This maximum likely occurred due to solute concentration during full freezing of the soil column in winter;
- A correlation between DOC, Al, Fe and trace elements element suggests control of organic complexes and colloids;
- Peat ice thaw can double the annual riverine export fluxes of DOC, P, and Zn in western Siberia

ABSTRACT

The physical and chemical consequences of massive ground ice (wedges) melt upon permafrost thaw is one of the central issues of environmental research linked to climate warming in the Arctic. Little is known about the chemical properties of dispersed ground ice abundant throughout permafrost peatlands that can easily melt with increasing active layer thickness (ALT). This is especially pertinent in continental lowlands, that account for sizeable areas of the Arctic, and contain high amount of organic carbon in both solid (peat) and liquid (porewater) phases. Here we studied 8 peat cores (0-130 cm depth)—comprised of porewater from the active layer (0-45 cm) as well as ice dispersed in frozen peat (40-130 cm)—across a latitudinal profile of Western Siberia Lowland (WSL) extending from discontinuous into continuous permafrost zones. Dissolved Organic Carbon (DOC), alkali and alkaline-earth metals (Ca, Mg, Sr, Ba, Li, Rb, Cs), sulfate, phosphorus, some trace elements (Al, Fe, Mn, Zn, Ni, Co, V, As, Y, REE, Zr, Hf, U) were sizably [more than 3 times] enriched in peat ice compared to peat porewaters from the active layer. In most sampled cores, there was a local maximum of strong enrichment (up to factors between 14 and 58) in DOC, P, Ca, Mg, Mn, Fe, Sr, As located 30-50 cm below the active layer. This maximum likely occurred due to solute concentration during full freezing of the soil column during winter. There was a sizable correlation between DOC, Al, Fe and other major and trace element concentrations that suggests strong control of organic complexes and organo-mineral (Al, Fe) colloids on element migration throughout the peat profile. The pool of C, major cations and trace metals in peat ice (40-130 cm) was approximately 3 to 55 times higher than the pool of these elements in porewaters from the active layer (0-40 cm). A 1-m increase of the ALT over the next 100 years is capable of mobilizing 58±38 Tg of DOC from soil ice into the rivers and lakes of the WSL latitudinal belt (63-67 °N). This fast lateral export of C (3.7±2.7 t C km^{-2} y^{-1}) may double current C yields in WSL rivers (3.4±1.3 t C km^{-2} y^{-1}). A strong increase (150 to 200 %) in riverine export of Zn, P and Cs may also occur while other micronutrients (Fe, Ni, Co, Ba, Mo, Rb) and toxicants (Cd, As, Al) may be affected to a lesser degree (20 to 30 % increase). We propose a global peat ice inventory in permafrost regions is essential for assessing the consequenaces of permafrost thaw on surface aquatic systems.

INTRODUCTION

Fast thawing of permafrost in the Arctic biome (Čapek et al., 2015; Grosse et al., 2016; Johnson et al., 2013; L. Pelletier et al., 2015; Luc Pelletier et al., 2015; Schuur et al., 2015; Vonk et al., 2015) brings about a number of events of local (thaw slumps, thermokarst, shore abrasion) and global (riverine water flux increase, C emission to the atmosphere and export to the Arctic Ocean) significance. In the majority of climate warming scenarios, thawing of frozen organic matter (OM) (Drake et al., 2015) and increase of hydrological flux and subsurface water travel time due to change of precipitation regime (Connolly et al., 2020; Frampton and Destouni, 2015; Walvoord and Kurylyk, 2016) are the main processes that have to be considered in predictive modeling of climate warming consequences in the Arctic. Dominant mechanisms for frozen OM transformation into aqueous DOC and greenhouse gases (CO_2, CH_4) include microbial and physico-chemical reactions of the solid C reservoir that is transferred into the aqueous and subsequently gaseous phase. In this regard, numerous studies have addressed the behavior of C and related elements during soil organic matter interaction with aqueous solutions and DOM transformation under biotic and abiotic processes (Drake et al., 2015; Shirokova et al., 2019; Vonk et al., 2013). Little attention has been given to the consequences of melting ground ice, capable of initiating rapid biotic and ecological changes, which can facilitate major ecosystem shifts (Becker et al., 2016; Parmentier et al., 2017; Selroos et al., 2019; Turetsky et al., 2020). Moreover, most studies of ground ice have dealt with massive ice lenses and wedges (Fritz et al., 2015, 2011; Opel et al., 2018; van Huissteden, 2020; Vonk et al., 2013) that are ubiquitous in continuous permafrost zones (French and Shur, 2010; French, 2007); however, such ice lenses and wedges may constitute only up to half of the volume of the top 3 m soil layer (Pollard and French, 1980). In contrast, dispersed ground ice present in soil pores beneath the active layer have remained outside of scientific research; these relatively small reservoirs of water, C and dissolved components are highly labile as they can thaw much faster. More importantly, dispersed ground ice exhibits strong enrichment in C and related elements, as has been demonstrated from the relatively limited studies concerning the yedoma soils (Ewing et al., 2015a; 2015b). Permafrost with low ice content (< 10%) occurs in mountainous regions and high

89 plateaus, and represents 15.8% of the land area (Zhang et al., 2008). Ground ice lenses and ice within
90 mineral soils have been extensively studied in permafrost soils of Northwestern Territories of
91 Canada (Kokelj et al., 2002; Kokelj and Burn, 2005, 2003), western Canadian Arctic (Subedi et al.,
92 2020), and in the Qinghai-Tibet Plateau (Wang et al., 2018), although these authors used distilled
93 water addition to characterize soil water chemical composition across the core. The importance of
94 studying soil ice in the permafrost regions stems from the fact that during summer most rivers and
95 lakes are fed via thawing of ground ice which is delivered to the hydrological network via
96 suprapermafrost flow (Loiko et al., 2019; Raudina et al., 2018; Thompson and Woo, 2009; Zong-Jie
97 et al., 2018).

98 Dispersed ice may be especially important in permafrost peatlands because of the high
99 porosity of peat and possibly the high vulnerability of ice located within discontinuous permafrost
100 zone. However, studies of chemical properties in native dispersed ice within peatlands of the
101 permafrost zone remain very limited. Furthermore, even porewater analyses from the active layer of
102 permafrost peatlands are very rare. In fact, among several studies of mineral soil porewaters from
103 permafrost regions (Fouché et al., 2014; Herndon et al., 2015; Jessen et al., 2014; Koch et al., 2013;
104 Marlin et al., 1993; Mavromatis et al., 2014; Pokrovsky et al., 2006; Prokushkin et al., 2005) only
105 Frey et al. (2016) and Raudina et al. (2017) provided such results. Frey et al. (2016) studied soil
106 pore waters from the yedoma wetland soil of the Kolyma River region. Raudina et al. (2017)
107 characterized peat porewater of the western Siberian Lowland (WSL). The lack of knowledge on the
108 chemical composition of soil ice in permafrost peatlands and pool of C and elements in this highly
109 labile solid phase is problematic. It can impede quantitative estimates on the consequences of active
110 layer deepening and permafrost thaw on C and element exportation from soil to river and ultimately
111 ocean.

112 This study aims to fill this knowledge gap by analyzing water and ice from several
113 representative peat core samples from the WSL, the largest permafrost peatland in the world. For this
114 study we sampled the interstitial soil solutions of the active layer and ice from frozen peat layers
115 across a 400-km latitudinal transect of discontinuous to continuous permafrost. In the context of

climate warming scenarios, understanding soil ice interactions within WSL is important due to the facts that: 1) it encompasses both discontinuous and continuous permafrost zones and contains soil temperatures around 0°C that are highly vulnerable to thawing (Romanovsky et al., 2010); 2) it contains a huge reservoir of organic carbon located in surficial (≤ 3-4 m) still frozen peat layers (Beilman et al., 2009; Botch et al., 1995; Frey and Smith, 2007; Gentsch et al., 2015; Kremenetski et al., 2003; Sheng et al., 2004; Tarnocai et al., 2009; Turunen et al., 2001); 3) the West Siberian peatlands contain the largest soil water and ice resources in the northern hemisphere (Smith et al., 2012); and 4) it presents a permafrost type gradient and highly homogeneous landscape parameters. The latter allows for straightforward testing of the effects of climate, permafrost, and vegetation on soil ice and water chemistry without interference from rock lithology, runoff, relief, proximity to the ocean, and localization of underground waters.

Our primary goal was to compare the distribution of Dissolved Organic Carbon (DOC), major and trace elements (TE) between pore waters and dispersed ice to evaluate the pools of C and inorganic solutes in liquid and frozen peat water. A secondary goal was to quantify the lateral pools of carbon and elements in these two highly mobile reservoirs of permafrost peatlands. For this, we analyzed the latitudinal trend of peat pore water and ice chemical composition with respect to DOC, major and TE concentration and we applied a substituting-space-for-time approach, originally developed for surface waters of western Siberia, (i.e. Frey et al., 2007a, 2007b; Frey and Smith, 2005). This allowed us providing empirical provisions on riverine export fluxes of C, nutrients and metals to the Arctic Ocean due to permafrost boundary change and the increase in active layer thickness.

2. Study site and Methods

2.1. Geographical setting and soil water and ice sampling

Several representative sites of permafrost peatlands (frozen bogs) were selected in the northern part of WSL as depicted in **Fig. 1.** These were comprised of 3 cores sampled in northern taiga (Khanymey), 3 peat cores sampled in forest-tundra (1 core in Pangody and 2 cores in Nadym),

and 2 cores sampled in southern tundra (Tazovsky) biomes. The region belongs to the watershed of the Ob, Nadym, Pur, and Taz rivers which drain Pleistocene sand and loess-like silts and are covered by a 0.1 to 4.0 m peat layer as described in **Table** 1. The mineral substrates are quite similar among all 4 sites of the northern part of WSL and were subjected to strong influence of aeolian and subaerial processes in the of the Late Pleistocene and Holocene (Astakhov and Nazarov, 2010; Panin et al., 2020; Velichko et al., 2011). Mean annual air temperatures are –5.6, –6.4, –5.7, and –9.1°C for Khanymey, Pandogy, Nadym and Tazovsky, respectively (Trofimova and Balybina, 2014). Permafrost is present at all sites and ranges from sporadic and discontinuous in the south to continuous in the north. The Khanymey, Pangody and Nadym sites were sampled exclusively on the peat mounds where the active layer thickness ranged from 28 to 45 cm. The annual temperature pattern at different depth of peat mound in the Khanymey site is shown in **Fig. 1 D.** In Tazovsky, permafrost is continuous which allowed for sampling thawed and frozen peat from both peat mound and hollow as the active (unfrozen) layer was always located within the peat horizon. The specificity of the WSL setting allows using a latitudinal approach to test the impact of permafrost on peat ice chemical composition as shown for peat waters (Raudina et al., 2017, 2018) because: 1) the boundaries of permafrost follow those of temperature and vegetation at otherwise similar relief, lithology and runoff; 2) we studied the most common Histosols that form large frozen peat bogs, occupying more than ¼ of the WSL territory (592,440 km²); and 3) all samples in this study were collected from frozen mounds, and we have demonstrated a subordinary role of local factors such as micro-landscapes on element concentration in peat porewaters (Raudina et al., 2017) and supra-permafrost waters (Raudina et al., 2018).

Altogether, 31 soil porous waters (from the active layer) and 66 peat ice (from the permafrost layer) in 4 sampling sites were collected from 5th-20th August 2018. To collect peat ice, the frozen peat core (diameter 4 cm) was extracted using a Russian peat borer (modified techniques according to Shary et al., 2018), cut using a ceramic blade into 10-cm layers, and thawed at room temperature. Immediately after full thawing of the frozen core, peat water was extracted through 100-µm precleaned Nylon net by applying a local confining pressure (1-5 kg cm^{-2}, depending on sample

humidity). The obtained slurry was centrifuged for 15 min at 3500 rpm and the supernatant was filtered through 0.45 µm acetate cellulose filter with the first 10 ml of filtrate discarded. The water from the thawed part of the peat core, above the permafrost table, was extracted using the same method but in the field and immediately after peat sampling. A similar procedure has been used for the yedoma ice characterization (Ewing et al., 2015a; 2015b). The ice content in permafrost peat layers was quantified by measuring the difference between the weight of a subsample (126 cm^3) of frozen core and its weight after full drying in an oven (for 2 days at 105°C).

2.2. Analyses

Filtered solutions were divided into two parts: 1) acidified (pH ~ 2) with ultrapure double-distilled HNO_3 for trace element (TE) analyses and 2) non-acidified for DOC, DIC and anion analyses. Blanks were performed to control the level of contamination induced by sampling and filtration. DOC blanks of filtrate never exceeded 0.2 mg/L which is quite low for the organic-rich waters sampled in this study (i.e., 10–200 mg/L DOC). The UV absorbance of the filtered samples was measured at 254 nm using 10-mm quartz cuvette on an Eppendorf BioSpectrometer. The specific UV-absorbency ($SUVA_{254}$, L $mg^{-1}m^{-1}$) is used as a proxy for aromatic C, molecular weight and source of DOM (Ilina et al., 2014; Weishaar et al., 2003).

The pH was measured in the field using a combined electrode with uncertainty of ±0.02 pH units. DOC and DIC were analyzed using a Carbon Total Analyzer (Shimadzu TOC VSCN) with an uncertainty better than 3% (see Prokushkin et al., 2011 for methodology). Major anion (Cl, SO_4^{2-}) concentrations were measured by ion chromatography (HPLC, Dionex ICS 2000) with an uncertainty of 2%. International certified samples ION, PERADE, and RAIN were used for validation of the analysis. Major cations (Ca, Mg, Na, K), Si, and ~40 trace elements were determined with an Agilent ce 7500 ICP-MS with In and Re as internal standards and 3 various external standards. Details of trace element analyses in DOC-rich waters of western Siberia can be found in Pokrovsky et al. (2016b). The SLRS-5 (Riverine Water Reference Material for Trace Metals certified by the National Research Council of Canada) was used to check accuracy and

reproducibility for each analysis (Yeghicheyan et al., 2013). Only those elements that exhibited good agreement between replicated measurements of SLRS-5 and the certified values (relative difference < 15%) are reported in this study.

2.3. Statistical treatment

The concentration of dissolved carbon and major and trace elements in peat waters at each sampling site was separately tested for normality. The normality of data distribution was explored using the Shapiro-Wilk test. Because data were not normally distributed, we used non-parametric statistics. Thus, the median and interquartile range (IQR) were used to trace dependence of element concentration on latitude in both the active layer and permafrost layer. Comparison of DOC, major and TE concentrations and pools in porewaters of the active layer and peat ice at each sampling site was conducted using a non-parametric Mann Whitney test at a significance level of 0.05. For comparison of unpaired data, a non-parametric H-criterion Kruskal-Wallis test was used to reveal the differences between different study sites.

Principal component analysis (PCA) was used for the full set of sampled waters and ice. The PCA analysis allowed to test the influence of various parameters, notably the latitude and ALT on the DOC and elemental concentrations. All graphics and figures were created using MS Excel 2010, MS Visio Professional 2016 and GS Grapher 11 package. Statistical treatment was performed using STATISTICA-7 (http://www.statsoft.com).

3. Results

3.1. PCA and correlations between elemental concentrations in peat porewater and ice

The PCA of the full dataset yielded 2 possible factors contributing to the observed variations in elemental concentrations (i.e., 24 and 15 %, **Fig. S1 of the Supplement**). The first factor acted on Be, Ti, V, Y, Zr, Nb, REE, Hf whereas the second factor was defined by DOC, SO_4^{2-}, Li, Mg, Al, Ca, Zn, Ga, Rb, Sr, Cd, Cs and Tl. A large number of elements yielded a significant ($R > 0.5$ at $p <$

0.05) and positive correlation with DOC such as SO_4, Li, Be, Mg, Al, P, Ca, Fe, Co, Ni, Ga, Rb, Sr, Cd, Cs and Tl for the full peat column (**Table S1 of the Supplement**). Considering the active and frozen part of the core separately, the DOC was positively ($p < 0.05$) correlated with Be, Al, Ni, Sr, Nb in the porewaters of the active layer and with SO_4^{2-}, Li, Be, Na, Mg, Al, Si, P, K, Ca, Mn, Fe, Co, Ni, Zn, Ga, Rb, Sr, Cd, Cs, Ba, Hf, Tl and Pb in the peat ice.

In the active layer porewaters, Fe always exhibited much lower correlation coefficients with most TE compared to Al. Thus, in the thawed layer, Al positively correlated ($R > 0.5$ at $p < 0.05$) with DOC, Li, Be, Si, Ca, Ti, V, Cr, Ni, Ga, Ge, Sr, Y, Zr, Nb, Mo, REE, Hf and U, whereas Fe correlated only with Si, Ca, Co, Ni and Sr. However, in the peat ice, virtually all major and trace elements correlated equally well ($R > 0.5$, $p < 0.05$) with both Fe and Al (**Table S1).**

3.2. Vertical profile of element concentration in active layer and frozen peat

The vertical concentration profiles of DOC, $SUVA_{254}$, P, Ca, Al, Fe, Na and Cl in sampled cores (porewater of peat active layer and permafrost peat ice) are illustrated in **Fig. 2 A-F**. Other elements are shown in Supplement **Fig. S2 and S3**. The mean values with S.D. for all major and trace elements in the active and frozen layers of each region, as well as the WSL-averaged values for peat porewater (ALT) and peat ice are listed in **Table 2**. Note that one Nadym core and one Khanymey core were sampled until 90-100 cm depth; although these cores are not illustrated in Fig. 2, the results were used for statistical treatment. According to the vertical pattern of element distribution from the surface downward to 90-130 cm peat depths, most major and trace elements exhibited concentrations in the active layer that were sizably (a factor of 2 to 10) lower than those in the frozen layer. The DOC, Ca, Mg, Sr, P, Fe, Mn, Li, Rb, Cs and As were mostly enriched in the peat ice and are 5 to 10 times the concentrations in the active layer. Only B, Cl, K, Sb and Pb demonstrated similar or even lower concentrations in peat ice when compared to the porewater. The $SUVA_{254}$ was always high above 60 cm depth, with the maximum values (2 to 4) achieved at 20-30 cm. A decrease in $SUVA_{254}$ with depth (below 30 cm) was pronounced in Khanymey, Nadym and Tazovsky peat cores.

There was a clearly pronounced local DOC peak that typically occurred 30-60 cm below the current active layer boundary (**Fig. 2 A, B, C, E, F**). It can be seen that this peak is highly pronounced in the Khanymey, Pangody and Tazovsky sites where DOC concentrations reached 1000, 1700, and 2400 mg/L, respectively. Some other major (Mg, Ca, Si, K) and trace (Li, Be, Al, P, Fe, V, Mn, Co, Ni, Zn, Ga, As, Rb, Sr, Mo, Cd, W and Pb) elements also exhibited a local maximum below the active layer (**Fig. 2** and **Fig. S3**).

To quantify this peak, we calculated the ratios of maximal concentration at the peak to the average value of the two nearest surface (0-10 and 10-20 cm depth) and the two deepest (130-120 cm and 120-110 cm) layers. A histogram illustrating the average ratios (degree of enrichment at the ~90 cm depth) and based on values averaged over all peat cores is shown in **Fig. 3**. It can be seen that Mn (by a factor of 12), DOC, Mg, Fe, Sr, P, Rb, Co, As, Cs, Li, Ni, SO_4, Cu, Hf, Be, Al, U, Zr, Cd, Y, V, Si, Tl, Zn and REEs are strongly (by a factor of 3 to 10) enriched in this layer relative to the surface horizons (**Fig. 3 B**). Phosphorus, Fe, DOC, Ca, Sr, SO_4^{2-}, Cs and U are enriched (by a factor of 2 to 5) in this layer relative to the bottom horizons of the peat core (**Fig. 3 C**).

3.3. Lateral elementary pools in active layer and permafrost layer

Based on water and ice content over the full depth of peat cores sampled across different permafrost zones, we calculated lateral (surface-normalized) pools of dissolved (< 0.45μm) C and elements in the upper active peat layer (0 to 30 cm depth depending on site), and in the bottom (frozen) peat layer (30 cm to 130 cm depth), as listed in **Table 3**. To calculate elementary pools in each layer under 1 m² of land surface, we used the equation:

$$[\text{Element Pool, g/m}^2] = C \times W$$

where C is average element concentration in the given layer, mg L^{-1}, and W is water content in the layer, L.

Two important observations can be made from these assessments. First, the pool of DOC, nutrients and metals in the peat ice is an order of magnitude (C, P, Ca, Mg, Fe, Al) or a factor of 2-5 (K, Si) higher than that in the pore water (**Fig. 4**). Despite the 3 times lesser thickness of the active

layer compared to the frozen peat, the difference is still significant for DOC, P, Ca, Mg, Fe and Al, suggesting preferential accumulation of these elements in peat ice. Second, there is no sizable latitudinal trend in either the porewater or the ice pool of C, P, K, Si and Fe. Only Ca and Mg demonstrated a northward increase in lateral stocks in both the 0-30 cm pore water and 30-130 cm peat ice [by a factor of 2-3 and 10, respectively]. However, many other trace elements (Li, Ca, V, Mn, Fe, Co, Ni, Zn, As, Rb, Sr, Y, Zr, Nb, Mo, Cd, Sb, REE, Hf, Pb and U) demonstrated really high concentrations, by at least a factor of 10, in the Tazovsky site (continuous permafrost zone) when compared to all three southern sites (sporadic and discontinuous permafrost zones) as shown from latitudinal patterns of relevant concentrations in the peat ice (**Fig. S4**). This produced quite high pools of relevant elements in the peat ice below ALT (**Table 2**).

4. Discussion

4.1. Organic carbon and Fe as main components of peat ice and carriers of elements in porewaters: freezing mechanisms controlling the vertical pattern of element concentration

Given the extremely high concentrations of DOC, Fe and Al in melted ice from peat cores (ca. 500, 2, and 0.8 mg L^{-1}, respectively), organic and organo-mineral (Fe, Al-rich) colloids are most likely carriers of most major (Ca and Mg) and trace elements, as it is known from surface waters of discontinuous permafrost peatland zones (Pokrovsky et al., 2016b; Krickov et al., 2019). As a result of such strong association of TE with DOC, Fe and Al, the behavior of virtually all solutes is controlled by processes involving colloid distribution between ice and remaining water during the freezing/thawing cycle of the peat water/ice. This is strongly confirmed by much higher correlations of DOC with major and trace elements in peat ice compared to active layer porewater (**Table S1**). It suggests that the the peat ice contains organo-mineral (Fe, Al) colloids where the proportion of Fe and Al is rather similar, as molar Fe to Al ratio in peat ice (< 0.45 µm fraction) across the WSL is close to 1 (**Table 2**). Similar to the surface waters of permafrost peatlands (Pokrovsky et al., 2016b), these high molecular weight colloids (10/100 kDa - 0.45 µm) contain sizable amounts of insoluble trace elements and are stabilized by organic matter. We hypothesize that peat ice colloids are formed

as a results of coprecipitation of TE with DOM-stabilized Fe and Al hydroxides as is known across the boreal zone in general (Cuss et al., 2018; Stolpe et al., 2013; Vasyukova et al., 2010) and in the WSL in particular (Krickov et al., 2019; Pokrovsky et al., 2016b). As a result of the dominance of Fe, Al-rich colloids in TE speciation in peat porewaters and peat ice, the concentrations of insoluble trace elements (trivalent and tetravalent hydrolysates, some heavy metals) were better correlated with Fe and Al rather than with DOC (**Table S1**). This is especially pronounced during filtration and ultrafiltration of surface waters from permafrost peatlands (Pokrovsky et al., 2016b) and calls for a need of size separation study on peat pore water and ice samples.

The quality of DOC changed from essentially aromatic, high $SUVA_{254}$ compounds in the thawed layer to more aliphatic, low chromophoric DOM (CDOM) character in the permafrost layer as follows from sizable decrease (a factor of 2 to 4) in $SUVA_{254}$ in the porewater of the active layer to the peat ice (**Fig. 2**). This is confirmed by a positive correlation between $SUVA_{254}$ and soil temperature ($R_{Spearman} = 0.48$, $p < 0.05$) as observed at the Khanymey site (**Table S2**). This can be explained by fresh DOC in deep frozen peat horizons and intensive biodegradation of DOC labile compounds in the active layer, leaving essentially aromatic DOC in the upper peat porewaters. Note also that the maximum of microbial metabolic activity and aliphatic DOC processing in studied peat cores (Khanymey site) was observed at the active layer-permafrost boundary (Morgalev et al., 2017). Peak DOC, nutrients, major and trace elements in the ice from the middle of the peat core is a particular and previously unknown feature of the WSL peatlands. Although the uneven distribution of solutes in permafrost soil ice has been known for long time, all available data concern mineral soils (sand, silt) and major cations and anions. For example, solute enrichment of near-surface permafrost with respect to the overlaying active layer yielding an increase with depth in soluble cation concentration was reported in the Mackenzie delta region (Kokelj and Burn, 2005), Herschel Island of the Canadian Arctic (Kokelj et al., 2002) and other Northwestern Territories (Kokelj and Burn, 2003). It was attributed to progressive removal of solutes from the active layer by advection and to convective transport of soluble materials along thermal gradients in near-surface permafrost

region (Kokelj and Burn, 2005) or removal and downward distribution of major ions during periods of deeper thaw at the end of summer (Burn and Michel, 1988; Kokelj and Burn, 2003).

The peak of concentration of DOC and elements in the peat ice was typically pronounced between 30 and 50 cm depth below the current active layer boundary. This was visible in 5 of 8 studied peat cores and suggests local freezing occurs throughout the year from both upper and bottom sections of the peat column; this is also confirmed by seasonal evolution of the temperature pattern in the peat profiles (see **Fig. 1**, bottom panel). The latter shows that in the end of the active seasons, starting from autumn, temperature decreases in both the upper and lowermost peat horizons. We therefore hypothesize that organic carbon and related elements, being present as organic and organo-mineral colloids, move together along the thermal gradient during soil freezing; this is known for major soluble ions (e.g. Cary and Mayland, 1972; Kokelj et al., 2002). As a result, two freezing fronts propagate and thereby concentrate the solutes—notably organic and organo-mineral colloids—in the unfrozen water layer and finally meet at some intermediate depth. This possibility is consistent with available natural and experimental data on bacteria translocations during freezing and thawing of peat cores from western Siberia (Morgalev et al., 2017, 2019).

We further hypothesize that the degree of hydrological confinement (i.e., the ability of squeezed peat water for lateral escape along the permafrost boundary towards depressions or thaw ponds) determines the presence or absence of C and solute maximum at the depth where these two freezing fronts meet each other. It can be hypothesized that the hydrological confinement did not occur in the bog of the Nadym site, which does not demonstrate a peak in element concentration below ALT. At the Nadym site, the hydrological regime can be described as a flowing fen rather than an ombrotrophic bog; furthermore, the hydrological connection (via suprapermafrost flow) between the mound and adjacent depression was much stronger than in other sites of this study. The latter could be linked to the larger amplitudes of height difference between mound and depressions in the Nadym that were observed in the field.

The latitudinal pattern of DOC and element concentration in peat ice was sizably different from that of peat porewaters of the active layer (this study and Raudina et al., 2017) and

358 suprapermafrost waters of the WSL (Raudina et al., 2018). The latter demonstrated an increase in
359 concentration of DOC, alkaline earth metals, Si, trivalent and tetravalent hydrolysates, and
360 micronutrients (Mn, Co, Ni, Cu, V and Mo) northward, with highest concentrations in the continuous
361 permafrost zone. In contrast, in peat ice, only Be, Mg, Ca, V, Mn, Fe, Co, Ni, Sr, Y, Zr, Mo, REE
362 and U demonstrated an increase in concentrations northward (**Table 2 and Fig. S4**). The
363 mechanisms responsible for DOC and other element concentrations increasing northward in fluids of
364 the active layer include peat leaching via its interaction with downward penetrating fluids and
365 atmospheric dust deposition as documented in recent studies of peat porewaters and suprapermafrost
366 flow (Raudina et al., 2017, 2018). Presumably, these mechanisms do not operate on ice dispersed
367 within the frozen peat. In the deeper parts of the core, well below the current ALT boundary, peat ice
368 either inherits the chemical signature of soil porewater from an environment which existed several
369 thousand years ago, not directly related to the current climate condition, or it represents the local
370 pattern of freezing front migration and solute concentration. In this regard, the representability of the
371 2-3 peat cores studied at each site may be an issue of concern given that the local ice content and its
372 chemical composition may be strongly controlled by disturbance events (Kokelj et al., 2002),
373 regional-scale landscape differences and solute translocations due to permafrost aggradation (Kokelj
374 and Burn, 2005).

375 Moreover, both the latitudinal and vertical pattern of solute concentrations in the dispersed
376 ice and the position of the DOC- and element-enriched layer in all studied peat cores may reflect the
377 localization of a paleo-active layer (of the mid Holocene), the thickness of which could be lower in
378 western Siberia than in other Arctic regions (125-130 cm in the MacKenzie Delta area Burn, 1997).
379 The difference in peat growth rates among bogs of the four study sites from various permafrost zones
380 may also explain the existence or lack of a DOC and solute maximum. For example, in the Nadym
381 site, there could potentially be two DOC maxima for the column (at 60-70 and 140 cm, see **Fig. 2 D**).
382 This would be consistent with the older age of this bog (~10,000 y.o., according to our ^{14}C
383 measurements). However, a detailed analysis of peat age, peat accumulation rate and the paleo-ALT
384 position is beyond the scope of this work. Another interesting observation was a sizable spatial

heterogeneity in the elementary composition of active layer water and peat ice which was dependent on the micro-landscape. Thus, the local maximum occurred in hollows about 30-40 cm deeper than in mounds (see **Fig. 2 E and F**). This is certainly controlled by local hydrology and the much deeper freezing/thawing of the depression compared to the mound (Kaverin et al., 2019; Loiko et al., 2019).

Overall, the concentrations of major and trace elements in peat ice studied in this work are sizably higher than those in other aquatic environments of the WSL. A Kruskall-Wallis test demonstrated that peat ice is significantly different from rivers (Pokrovsky et al., 2016a), lakes (Manasypov et al., 2020), and supra-permafrost waters (Raudina et al., 2018) in all major and trace elements (**Fig. S5)**. Concentrations of Co, V, Mo, Li, K, Tl, U, Cs, Sr, As, DIC, Cl-, DOC, Ca, Mg W, Rb, Ba, Na and SO_4^{2-} are 2 to 12 times higher in the peat ice compared to supra-permafrost waters where as the concentrations of B and Zn are a factor of 21 and 26 higher (**Table S3**). The river waters are impoverished in Th, As, Ga, Co, Cd, Rb, Zn, Al, Cs, DOC compared to peat ice by a factor of 10 to 70, whereas the concentrations of Fe, Cr, Ca, Pb, K, Sb, Ba, Cu, Ni, Mo, Zr, B, Ti, V, U and REEs in peat ice are higher than those in rivers by a factor of 2 to 9. Compared to lake waters, the peat ice is enriched in all elements by a factor of 2 to 50; this enrichment is most pronounced for Co, Si, K, DOC, Zn, SO_4^{2-}, Cs, P, W, and Rb (x 10 to 50).

4.2. Pools of C and other elements in dispersed peat ice of the WSL and possible consequences of permafrost thaw on riverine export

According to typical scenario of climate warming impact on western Siberian peatlands, there will be a northward retreat of the permafrost boundary and an increase in the ALT (Anisimov et al., 2013; Frey and Smith, 2003; Nitzbon et al., 2020; Pavlov and Moskalenko, 2002; Reshetko and Moiseeva, 2016; Romanovsky et al., 2010; Sherstyukov and Sherstyukov, 2015; Vasiliev et al., 2020a, b, 2011). The primary impact of permafrost thaw on element mobilization from soil ice to the hydrological network is involvement of larger amount of frozen peat during seasonal thawing triggered by an increase in ALT due to progressive thawing of ground ice. According to most recent data of Vasiliev et al. (2020b), during the period 1970-2018, the mean annual air temperature raised

412 by 2.8°C, the precipitation increased by 5-10%, and the mean height of snow cover increased by 1.8
413 cm y^{-1}. This led to an increase in average temperature of permafrost in Siberia by 0.035-0.056 °C y^{-1}
414 whereas the ALT increased with a range of rate from a few cm to several decimeters per year
415 depending on landscape context, vegetation cover and soil substrates. For example, well drained
416 regions of mineral soils during some years of high precipitation may exhibit the rates as high as 20-
417 40 cm y^{-1} (Vasiliev et al., 2020b). Note that these rates are sizably higher than those of Northern
418 Sweden where similar palsa peatbogs thaw with an average rate of 1 cm per year (Åkerman and
419 Johansson, 2008; Johansson et al., 2011). However, in the estimations below we will use the most
420 conservative scenario of 1 cm y^{-1}.

421 Considering the minimal rate of ALT increase in western Siberia, over the next 100 years,
422 about 1 m of frozen peat will thaw and liberate the solutes of dispersed ice to the hydrological
423 network. Assuming conservative transfer of these solutes from the soil to the river, a sizable amount
424 of elements can be added to the riverine export flux. For example, average pools of DOC, P and Fe
425 in the dispersed peat ice between 30 and 130 cm depth equal 369, 1, and 1.7 g m^{-2}; a progressive
426 thawing of 1 m of frozen peat during 100 years will liberate 3.69, 0.01 and 0.17 g m^{-2} y^{-1},
427 respectively, of these elements from the soil to the river. These values are comparable or higher than
428 the actual yields of DOC, P and Fe by permafrost-affected WSL rivers to the Arctic Ocean (3.4±1.3,
429 0.0057±0.002, and 0.092±0.04 g m^{-2} y^{-1}, Pokrovsky et al., 2020).

430 Furthermore, many other elements including macro- and micro-nutrients and toxicants are
431 strongly enriched in the peat ice of the continuous permafrost zones compared to the discontinuous
432 and sporadic zones. Progressive thawing of peat columns to over 100 cm depth is capable of
433 liberating a sizable amount of these trace elements that will be delivered to the hydrological network.
434 The area-normalized yields of elements from thawing of peat ice are comparable or higher than the
435 contemporary lateral export fluxes by rivers from the permafrost-affected WSL zone (Pokrovsky et
436 al., 2020). Assuming that the thawing of peat ice will add additional elements to the 'constant'
437 riverine export and neglecting possible reactivity of newly thawed peat, gradual thawing of frozen
438 layer (1 cm y^{-1}) will double or triple the annual riverine export of DOC, Zn, P and Cs for the next

100 years (**Table 4**). The lateral export of Co, Ba, Cd, As, Al, Rb, Ga and Mo may increase by 20 to 40% whereas for Fe, Ni, SO_4, U, Pb, Nb, B this increase may be between 10 to 20%. All other elements will be weakly (< 10%) affected by peat ice thaw.

5. Concluding remarks

The first study of ice dispersed within the frozen peat layers of the permafrost peatland in Western Siberia revealed sizeable—by a factor of 3 to 10—enrichment of the permafrost layer relative to the thawed layer in DOC, alkali, alkaline earth elements, metal micronutrients and geochemical tracers. The quality of DOC also changed from an essentially aromatic high SUVA compounds in the thawed layer to a more aliphatic low-CDOM compounds in the permafrost layer. This can be explained by fresh DOC in the deep frozen peat horizons and intensive biodegradation of DOC labile compounds in the active layer, leaving essentially aromatic DOC in upper soil porewaters. The concentrations of DOC, Fe and Al were correlated in both porewaters of the active layer and in the peat ice suggesting that organic and organo-mineral colloids are the main carriers of most solutes in the interstitial fluids of peat cores.

We discovered a strong local maximum of DOC, P, Ca, Fe and other trace element concentrations in ice sampled at 30 to 50 cm depth below the current active layer boundary. This enrichment at 90±10 cm depth was pronounced in all peat cores of the frozen mounds in sporadic, discontinuous and continuous permafrost zones and it was presumably formed due to freezing of the soil column from both the surface and bottom leading to a mid-point joint freezing process thereby concentrating the solute. In depressions this maximum was located 20-30 cm deeper than in mounds and reflected much high ALT in the former. This resulted from differences in water migration across microlandscapes.

Pools of DOC and elements located in peat ice dispersed within the 30-130 cm frozen layer were a factor of 3 to 10 higher than those within the active layer itself. Pools of most elements were not sizably different among various permafrost zones and latitudes. Thus, the permafrost boundary shift northward might not strongly affect mobile pools of DOC and elements in peat porewaters and

ice. However, assuming permafrost thaw scenarios with ALT increase by 1 cm y^{-1}, a sizable amount of highly labile C and related elements can be mobilized from currently frozen peat into the hydrological network via the suprapermafrost flow. When comparing with contemporary export fluxes of C and elements by WSL rivers in discontinuous and continuous permafrost zones, thaw of 100 cm of frozen peat over the next 100 years may at least double the annual delivery of DOC and some nutrients (P and Zn) to the Arctic Ocean.

Data availability: The full data set of measured DOC, major and trace element concentrations (< 0.45 μm) in the peat poreater from the active and ice from frozen layer in all sites and different sampling depths is presented in the Mendeley portal database (Lim et al., 2020).

Acknowledgements

We acknowledge support from Russian Science Foundation (RSF) grant No 18-77-10045 for field and laboratory work, laboratory and data analysis, and Russian Foundation for Basic Research (grants Nos 19-29-05209-mk, 19-55-15002 and 20-05-00729_a). We are grateful to G. Istigechev for help with producing figure Fig. 1D. C. Benker is thanked for editing the English of the manuscript. We are grateful to two anonymous reviewers for very constructive comments.

References

Åkerman, H.J., Johansson, M., 2008. Thawing permafrost and thicker active layers in sub-arctic Sweden. Permafr. Periglac. Process. 19, 279–292. https://doi.org/10.1002/ppp.626

Anisimov, O., Kokorev, V., Zhil'tsova, Y., 2013. Temporal and spatial patterns of modern climatic warming: Case study of Northern Eurasia. Clim. Change 118, 871–883. https://doi.org/10.1007/s10584-013-0697-4

Astakhov, V., Nazarov, D., 2010. Correlation of Upper Pleistocene sediments in northern West Siberia. Quat. Sci. Rev. 29, 3615–3629. https://doi.org/10.1016/j.quascirev.2010.09.001

Becker, M.S., Davies, T.J., Pollard, W.H., 2016. Ground ice melt in the high Arctic leads to greater ecological heterogeneity. J. Ecol. 104, 114–124. https://doi.org/10.1111/1365-2745.12491

Beilman, D.W., MacDonald, G.M., Smith, L.C., Reimer, P.J., 2009. Carbon accumulation in peatlands of West Siberia over the last 2000 years. Global Biogeochem. Cycles 23. https://doi.org/10.1029/2007GB003112

Botch, M.S., Kobak, K.I., Vinson, T.S., Kolchugina, T.P., 1995. Carbon pools and accumulation in peatlands of the former Soviet Union. Global Biogeochem. Cycles 9, 37–46. https://doi.org/10.1029/94GB03156

Burn, C.R., 1997. Cryostratigraphy, paleogeography, and climate change during the early Holocene warm interval, western Arctic coast, Canada. Can. J. Earth Sci. 34, 912–925. https://doi.org/https://doi.org/10.1139/e17-076

Burn, C.R., Michel, F.A., 1988. Evidence for recent temperature-induced water migration into permafrost from the tritium content of ground ice near Mayo, Yukon Territory, Canada. Can. J. Earth Sci. 25, 909–915. https://doi.org/10.1139/e88-087

Čapek, P., Diáková, K., Dickopp, J.E., Bárta, J., Wild, B., Schnecker, J., Alves, R.J.E., Aiglsdorfer, S., Guggenberger, G., Gentsch, N., Hugelius, G., Lashchinsky, N., Gittel, A., Schleper, C., Mikutta, R., Palmtag, J., Shibistova, O., Urich, T., Richter, A., Šantrůčková, H., 2015. The effect of warming on the vulnerability of subducted organic carbon in arctic soils. Soil Biol. Biochem. 90, 19–29. https://doi.org/10.1016/j.soilbio.2015.07.013

Cary, J.W., Mayland, H.F., 1972. Salt and Water Movement in Unsaturated Frozen Soil. Soil Sci. Soc. Am. J. 36, 549–555. https://doi.org/10.2136/sssaj1972.03615995003600040019x

Connolly, C.T., Cardenas, M.B., Burkart, G.A., Spencer, R.G.M., McClelland, J.W., 2020. Groundwater as a major source of dissolved organic matter to Arctic coastal waters. Nat. Commun. 11, 1–8. https://doi.org/10.1038/s41467-020-15250-8

Cuss, C.W., Donner, M.W., Grant-Weaver, I., Noernberg, T., Pelletier, R., Sinnatamby, R.N., Shotyk, W., 2018. Measuring the distribution of trace elements amongst dissolved colloidal species as a fingerprint for the contribution of tributaries to large boreal rivers. Sci. Total Environ. 642, 1242–1251. https://doi.org/10.1016/j.scitotenv.2018.06.099

Drake, T.W., Wickland, K.P., Spencer, R.G.M., McKnight, D.M., Striegl, R.G., 2015. Ancient low-molecular-weight organic acids in permafrost fuel rapid carbon dioxide production upon thaw. Proc. Natl. Acad. Sci. U. S. A. 112, 13946–13951. https://doi.org/10.1073/pnas.1511705112

Ewing, S. A., O'Donnell, J.A., Aiken, G.R., Butler, K., Butman, D., Windham-Myers, L., Kanevskiy, M.Z., 2015a. Long-term anoxia and release of ancient, labile carbon upon thaw of Pleistocene permafrost. Geophys. Res. Lett. 42, 10730–10738. https://doi.org/10.1002/2015GL066296

Ewing, S. A., Paces, J.B., O'Donnell, J.A., Jorgenson, M.T., Kanevskiy, M.Z., Aiken, G.R., Shur, Y., Harden, J.W., Striegl, R., 2015b. Uranium isotopes and dissolved organic carbon in loess permafrost: Modeling the age of ancient ice. Geochim. Cosmochim. Acta 152, 143–165. https://doi.org/10.1016/j.gca.2014.11.008

Fouché, J., Keller, C., Allard, M., Ambrosi, J.P., 2014. Increased CO2 fluxes under warming tests and soil solution chemistry in Histic and Turbic Cryosols, Salluit, Nunavik, Canada. Soil Biol. Biochem. 68, 185–199. https://doi.org/10.1016/j.soilbio.2013.10.007

Frampton, A., Destouni, G., 2015. Impact of degrading permafrost on subsurface solute transport pathways and travel times. Water Resour. Res. 51, 7680–7701. https://doi.org/10.1002/2014WR016689

French, H., Shur, Y., 2010. The principles of cryostratigraphy. Earth-Science Rev. 101, 190–206. https://doi.org/10.1016/j.earscirev.2010.04.002

French, H.M., 2007. The Periglacial Environment, 3rd ed. John Wiley and Sons Ltd, West Sussex, England.

Frey, K.E., McClelland, J.W., Holmes, R.M., Smith, L.G., 2007a. Impacts of climate warming and permafrost thaw on the riverine transport of nitrogen and phosphorus to the Kara Sea. J. Geophys. Res. Biogeosciences 112. https://doi.org/10.1029/2006JG000369

Frey, K.E., Siegel, D.I., Smith, L.C., 2007b. Geochemistry of west Siberian streams and their potential response to permafrost degradation. Water Resour. Res. 43. https://doi.org/10.1029/2006WR004902

Frey, K.E., Smith, L.C., 2007. How well do we know northern land cover? Comparison of four global vegetation and wetland products with a new ground-truth database for West Siberia. Global Biogeochem. Cycles 21. https://doi.org/10.1029/2006GB002706

Frey, K.E., Smith, L.C., 2005. Amplified carbon release from vast West Siberian peatlands by 2100. Geophys. Res. Lett. 32, 1–4. https://doi.org/10.1029/2004GL022025

Frey, K.E., Smith, L.C., 2003. Recent temperature and precipitation increases in West Siberia and their association with the Arctic Oscillation. Polar Res. 22, 287–300. https://doi.org/10.1111/j.1751-8369.2003.tb00113.x

Frey, K.E., Sobczak, W. V., Mann, P.J., Holmes, R.M., 2016. Optical properties and bioavailability

of dissolved organic matter along a flow-path continuum from soil pore waters to the Kolyma River mainstem, East Siberia. Biogeosciences 13, 2279–2290. https://doi.org/10.5194/bg-13-2279-2016

Fritz, M., Opel, T., Tanski, G., Herzschuh, U., Meyer, H., Eulenburg, A., Lantuit, H., 2015. Dissolved organic carbon (DOC) in Arctic ground ice. Cryosph. Discuss. 9, 77–114. https://doi.org/10.5194/tcd-9-77-2015

Fritz, M., Wetterich, S., Meyer, H., Schirrmeister, L., Lantuit, H., Pollard, W.H., 2011. Origin and characteristics of massive ground ice on Herschel Island (western Canadian Arctic) as revealed by stable water isotope and Hydrochemical signatures. Permafr. Periglac. Process. 22, 26–38. https://doi.org/10.1002/ppp.714

Gentsch, N., Mikutta, R., Alves, R.J.E., Barta, J., Čapek, P., Gittel, A., Hugelius, G., Kuhry, P., Lashchinskiy, N., Palmtag, J., Richter, A., Šantrůčková, H., Schnecker, J., Shibistova, O., Urich, T., Wild, B., Guggenberger, G., 2015. Storage and transformation of organic matter fractions in cryoturbated permafrost soils across the Siberian Arctic. Biogeosciences 12, 4525–4542. https://doi.org/10.5194/bg-12-4525-2015

Grosse, G., Goetz, S., McGuire, A.D., Romanovsky, V.E., Schuur, E.A., 2016. Changing permafrost in a warming world and feedbacks to the Earth system. Environ. Res. Lett. 11. https://doi.org/10.1088/1748-9326/11/4/040201

Herndon, E.M., Dere, A.L., Sullivan, P.L., Norris, D., Reynolds, B., Brantley, S.L., 2015. Landscape heterogeneity drives contrasting concentration-discharge relationships in shale headwater catchments. Hydrol. Earth Syst. Sci. 19, 3333–3347. https://doi.org/10.5194/hess-19-3333-2015

Ilina, S.M., Drozdova, O.Y., Lapitskiy, S.A., Alekhin, Y. V., Demin, V. V., Zavgorodnyaya, Y.A., Shirokova, L.S., Viers, J., Pokrovsky, O.S., 2014. Size fractionation and optical properties of dissolved organic matter in the continuum soil solution-bog-river and terminal lake of a boreal watershed. Org. Geochem. 66, 14–24. https://doi.org/10.1016/j.orggeochem.2013.10.008

Jessen, S., Holmslykke, H.D., Rasmussen, K., Richardt, N., Holm, P.E., 2014. Hydrology and pore water chemistry in a permafrost wetland, Ilulissat, Greenland. Water Resour. Res. 50, 4760–4774. https://doi.org/10.1002/2013WR014376

Johansson, M., Åkerman, J., Keuper, F., Christensen, T.R., Lantuit, H., Callaghan, T. V., 2011. Past and present permafrost temperatures in the Abisko area: Redrilling of boreholes. Ambio 40, 558–565. https://doi.org/10.1007/s13280-011-0163-3

Johnson, K.D., Harden, J.W., McGuire, A.D., Clark, M., Yuan, F., Finley, A.O., 2013. Permafrost and organic layer interactions over a climate gradient in a discontinuous permafrost zone. Environ. Res. Lett. 8. https://doi.org/10.1088/1748-9326/8/3/035028

Kaverin, D.A., Pastukhov, A. V, Novakovsky, A.B., Biasi, K., Marushchak, M., Elsakov, V. V, 2019. Landscape and climatic factors impacting the thaw depth in soils of permafrost peat plateaus (on the example of CALM r52 site). Kriosf. Zemli XXIII, 53–60. https://doi.org/10.21782/EC2541-9994-2019-2(53-60)

Koch, J.C., Runkel, R.L., Striegl, R., McKnight, D.M., 2013. Hydrologic controls on the transport and cycling of carbon and nitrogen in a boreal catchment underlain by continuous permafrost. J. Geophys. Res. Biogeosciences 118, 698–712. https://doi.org/10.1002/jgrg.20058

Kokelj, S. V., Burn, C.R., 2005. Geochemistry of the active layer and near-surface permafrost, Mackenzie delta region, Northwest Territories, Canada. Can. J. Earth Sci. 42, 37–48. https://doi.org/10.1139/E04-089

Kokelj, S. V., Burn, C.R., 2003. Ground ice and soluble cations in near-surface permafrost, Inuvik, Northwest Territories, Canada. Permafr. Periglac. Process. 14, 275–289. https://doi.org/10.1002/ppp.458

Kokelj, S. V., Smith, C.A.S., Burn, C.R., 2002. Physical and chemical characteristics of the active layer and permafrost, Herschel Island, western Arctic Coast, Canada. Permafr. Periglac. Process. 13, 171–185. https://doi.org/10.1002/ppp.417

Kremenetski, K. V., Velichko, A.A., Borisova, O.K., MacDonald, G.M., Smith, L.C., Frey, K.E., Orlova, L.A., 2003. Peatlands of the Western Siberian lowlands: Current knowledge on zonation, carbon content and Late Quaternary history. Quat. Sci. Rev. 22, 703–723.

https://doi.org/10.1016/S0277-3791(02)00196-8
Krickov, I.V., Pokrovsky, O.S., Manasypov, R.M., Lim, A.G., Shirokova, L.S., Viers, J., 2019. Colloidal transport of carbon and metals by western Siberian rivers during different seasons across a permafrost gradient. Geochim. Cosmochim. Acta 265, 221–241. https://doi.org/10.1016/j.gca.2019.08.041
Lim, A.G., Loiko, S.V., Kuzmina, D.M., Shirokova, L.S., Kulizhsky, S.P., Pokrovsky, O.S. 2020. Elements concentration in peat ice and porewaters across the permafrost gradient of Western Siberia, Mendeley Data, v2. DOI: 10.17632/hkzvkhdbyw.1.
Loiko, S.V., Raudina, T.V., Lim, A.G., Kuzmina, D.M., Kulizhskiy, S.P., Pokrovsky, O.S., 2019. Microtopography controls of carbon and related elements distribution in the West Siberian frozen bogs. Geosciences 9, 291. https://doi.org/10.3390/geosciences9070291
Manasypov, R.M., Lim, A.G., Krickov, I. V., Shirokova, L.S., Vorobyev, S.N., Kirpotin, S.N., Pokrovsky, O.S., 2020. Spatial and seasonal variations of C, nutrient, and metal concentration in thermokarst lakes of Western Siberia across a permafrost gradient. Water 12, 1830. https://doi.org/10.3390/w12061830
Marlin, C., Dever, L., Vachier, P., Courty, M.A., 1993. Chemical and isotopic changes in soil-water during refrosting of an active layer on continuous permafrost (Brogger-peninsula, Svalbard). Can. J. Earth Sci. 30, 806–813.
Mavromatis, V., Prokushkin, A.S., Pokrovsky, O.S., Viers, J., Korets, M.A., 2014. Magnesium isotopes in permafrost-dominated Central Siberian larch forest watersheds. Geochim. Cosmochim. Acta 147, 76–89. https://doi.org/10.1016/j.gca.2014.10.009
Morgalev, S.Y., Morgaleva, T.G., Morgalev, Y.N., Loiko, S. V, Manasypov, R.M., Lim, A.G., Pokrovsky, O.S., 2019. Experimental modeling of the bacterial community translocation during freezing and thawing of peat permafrost soils of Western Siberia. IOP Conf. Ser. Earth Environ. Sci. 400, 12017. https://doi.org/10.1088/1755-1315/400/1/012017
Morgalev, Y.N., Lushchaeva, I. V., Morgaleva, T.G., Kolesnichenko, L.G., Loiko, S. V., Krickov, I. V., Lim, A., Raudina, T.V., Volkova, I.I., Shirokova, L.S., Morgalev, S.Y., Vorobyev, S.N., Kirpotin, S.N., Pokrovsky, O.S., 2017. Bacteria primarily metabolize at the active layer/permafrost border in the peat core from a permafrost region in western Siberia. Polar Biol. 40, 1645–1659. https://doi.org/10.1007/s00300-017-2088-1
Nitzbon, J., Westermann, S., Langer, M., Martin, L.C.P., Strauss, J., Laboor, S., Boike, J., 2020. Fast response of cold ice-rich permafrost in northeast Siberia to a warming climate. Nat. Commun. 11, 1–11. https://doi.org/10.1038/s41467-020-15725-8
Opel, T., Meyer, H., Wettericj, S., Laepple, T., Dereviagin, A., Murton, J., 2018. Ice wedges as archives of winter paleoclimate: a review. Permafrost Periglacial Process. 29(3), 199-209. https://doi.org/10.1002/ppp.1980.
Panin, A. V., Astakhov, V.I., Lotsari, E., Komatsu, G., Lang, J., Winsemann, J., 2020. Middle and Late Quaternary glacial lake-outburst floods, drainage diversions and reorganization of fluvial systems in northwestern Eurasia. Earth-Science Rev. https://doi.org/10.1016/j.earscirev.2019.103069
Parmentier, F. W., Christensen, T. R., Rysgaard, S. et al., 2017. A synthesis of the arctic terrestrial and marine carbon cycles under pressure from a dwindling cryosphere. Ambio 46, 53–69. https://doi.org/10.1007/s13280-016-0872-8
Pavlov, A. V., Moskalenko, N.G., 2002. The thermal regime of soils in the north of Western Siberia. Permafr. Periglac. Process. 13, 43–51. https://doi.org/10.1002/ppp.409
Pelletier, L., Strachan, I.B., Roulet, N.T., Garneau, M., 2015. Can boreal peatlands with pools be net sinks for CO2? Environ. Res. Lett. 10, 035002. https://doi.org/10.1088/1748-9326/10/3/035002
Pelletier, Luc, Strachan, I.B., Roulet, N.T., Garneau, M., Wischnewski, K., 2015. Effect of open water pools on ecosystem scale surface-atmosphere carbon dioxide exchange in a boreal peatland. Biogeochemistry 124, 291–304. https://doi.org/10.1007/s10533-015-0098-z
Pokrovsky, O.S., Manasypov, R.M., Kopysov, S.G., Krickov, I. V., Shirokova, L.S., Loiko, S. V., Lim, A.G., Kolesnichenko, L.G., Vorobyev, S.N., Kirpotin, S.N., 2020. Impact of Permafrost Thaw and Climate Warming on Riverine Export Fluxes of Carbon, Nutrients and Metals in

Western Siberia. Water 12, 1817. https://doi.org/10.3390/w12061817
Pokrovsky, O.S., Manasypov, R.M., Loiko, S. V., Krickov, I.A., Kopysov, S.G., Kolesnichenko, L.G., Vorobyev, S.N., Kirpotin, S.N., 2016a. Trace element transport in western Siberian rivers across a permafrost gradient. Biogeosciences 13, 1877–1900. https://doi.org/10.5194/bg-13-1877-2016
Pokrovsky, O.S., Manasypov, R.M., Loiko, S. V., Shirokova, L.S., 2016b. Organic and organo-mineral colloids in discontinuous permafrost zone. Geochim. Cosmochim. Acta 188, 1–20. https://doi.org/10.1016/j.gca.2016.05.035
Pokrovsky, O.S., Schott, J., Dupré, B., 2006. Trace element fractionation and transport in boreal rivers and soil porewaters of permafrost-dominated basaltic terrain in Central Siberia. Geochim. Cosmochim. Acta 70, 3239–3260. https://doi.org/10.1016/j.gca.2006.04.008
Pokrovsky, O.S., Shirokova, L.S., Kirpotin, S.N., Kulizhsky, S.P., Vorobiev, S.N., 2013. Effects of anomalous high temperatures on carbon dioxide, methane, dissolved organic carbon and trace element concentrations in thaw lakes in Western Siberia in 2012. Biogeosciences Discuss. 10, 7257–7297. https://doi.org/10.5194/bgd-10-7257-2013
Pollard, W.H., French, H.M., 1980. A first approximation of the volume of ground ice, Richards Island, Pleistocene Mackenzie delta, Northwest Territories, Canada. Can. Geotech. J. 17, 509–516. https://doi.org/10.1139/t80-059
Prokushkin, A.S., Kajimoto, T., Prokushkin, S.G., McDowell, W.H., Abaimov, A.P., Matsuura, Y., 2005. Climatic factors influencing fluxes of dissolved organic carbon from the forest floor in a continuous-permafrost Siberian watershed. Can. J. For. Res. 35, 2130–2140. https://doi.org/10.1139/x05-150
Prokushkin, A.S., Pokrovsky, O.S., Shirokova, L.S., Korets, M.A., Viers, J., Prokushkin, S.G., Amon, R.M.W., Guggenberger, G., Mcdowell, W.H., 2011. Sources and the flux pattern of dissolved carbon in rivers of the Yenisey basin draining the Central Siberian Plateau. Environ. Res. Lett. 6, 45212–45226. https://doi.org/10.1088/1748-9326/6/4/045212
Raudina, T. V., Loiko, S. V., Lim, A.G., Krickov, I. V., Shirokova, L.S., Istigechev, G.I., Kuzmina, D.M., Kulizhsky, S.P., Vorobyev, S.N., Pokrovsky, O.S., 2017. Dissolved organic carbon and major and trace elements in peat porewater of sporadic, discontinuous, and continuous permafrost zones of western Siberia. Biogeosciences 14, 3561–3584. https://doi.org/10.5194/bg-14-3561-2017
Raudina, T. V., Loiko, S. V., Lim, A., Manasypov, R.M., Shirokova, L.S., Istigechev, G.I., Kuzmina, D.M., Kulizhsky, S.P., Vorobyev, S.N., Pokrovsky, O.S., 2018. Permafrost thaw and climate warming may decrease the CO_2, carbon, and metal concentration in peat soil waters of the Western Siberia Lowland. Sci. Total Environ. 634, 1004–1023. https://doi.org/10.1016/j.scitotenv.2018.04.059
Reshetko, M. V., Moiseeva, Y.A., 2016. Climatic features and statistical evaluation of climate change in permafrost regions in the north of western Siberia. Bull. Tomsk Polytech. Univ. 327, 108-118 (In russian).
Romanovsky, V.E., Drozdov, D.S., Oberman, N.G., Malkova, G. V., Kholodov, A.L., Marchenko, S.S., Moskalenko, N.G., Sergeev, D.O., Ukraintseva, N.G., Abramov, A.A., Gilichinsky, D.A., Vasiliev, A.A., 2010. Thermal state of permafrost in Russia. Permafr. Periglac. Process. 21, 136–155. https://doi.org/10.1002/ppp.683
Schuur, E.A.G., McGuire, A.D., Schädel, C., Grosse, G., Harden, J.W., Hayes, D.J., Hugelius, G., Koven, C.D., Kuhry, P., Lawrence, D.M., Natali, S.M., Olefeldt, D., Romanovsky, V.E., Schaefer, K., Turetsky, M.R., Treat, C.C., Vonk, J.E., 2015. Climate change and the permafrost carbon feedback. Nature. https://doi.org/10.1038/nature14338
Selroos, J.-O., Cheng, H., Vidstrand, P., Destouni, G., 2019. Permafrost Thaw with Thermokarst Wetland-Lake and Societal-Health Risks: Dependence on Local Soil Conditions under Large-Scale Warming. Water 11, 574. https://doi.org/10.3390/w11030574
Shary, P.A., Sharaya, L.S., Pastukhov, A. V., Kaverin, D.A., 2018. Spatial distribution of organic carbon in soils of Eastern European tundra and forest-tundra depending on climate and topography. Izv. Ross. Akad. Nauk. Seriya Geogr. 2018, 39-48 (In russian).

https://doi.org/10.1134/S2587556618060146
Sheng, Y., Smith, L.C., MacDonald, G.M., Kremenetski, K. V., Frey, K.E., Velichko, A.A., Lee, M., Beilman, D.W., Dubinin, P., 2004. A high-resolution GIS-based inventory of the west Siberian peat carbon pool. Global Biogeochem. Cycles 18. https://doi.org/10.1029/2003GB002190
Sherstyukov, A.B., Sherstyukov, B.G., 2015. Spatial features and new trends in thermal conditions of soil and depth of its seasonal thawing in the permafrost zone. Russ. Meteorol. Hydrol. 40, 73–78. https://doi.org/10.3103/S1068373915020016
Shirokova, L.S., Chupakov, A., Zabelina, S., Neverova, N., Payandi-Rolland, D., Causserand, C., Karlsson, J., Pokrovsky, O.S., 2019. Humic surface waters of frozen peat bogs (permafrost zone) are highly resistant to bio- and photodegradation. Biogeosciences 16, 2511–2526. https://doi.org/10.5194/bg-16-2511-2019
Smith, L.C., Beilman, D.W., Kremenetski, K. V., Sheng, Y., MacDonald, G.M., Lammers, R.B., Shiklomanov, A.I., Lapshina, E.D., 2012. Influence of permafrost on water storage in West Siberian peatlands revealed from a new database of soil properties. Permafr. Periglac. Process. 23, 69–79. https://doi.org/10.1002/ppp.735
Stolpe, B., Guo, L., Shiller, A.M., Aiken, G.R., 2013. Abundance, size distributions and trace-element binding of organic and iron-rich nanocolloids in Alaskan rivers, as revealed by field-flow fractionation and ICP-MS. Geochim. Cosmochim. Acta 105, 221–239. https://doi.org/10.1016/j.gca.2012.11.018
Subedi, R., Kokelj, S. V., Gruber, S., 2020. Ground ice, organic carbon and soluble cations in tundra permafrost and active-layer soils near a Laurentide ice divide in the Slave Geological Province, N.W.T., Canada. The Cryosphere, https://doi.org/10.5194/tc-2020-33.
Tarnocai, C., Canadell, J.G., Schuur, E.A.G., Kuhry, P., Mazhitova, G., Zimov, S., 2009. Soil organic carbon pools in the northern circumpolar permafrost region. Global Biogeochem. Cycles 23, 1–11. https://doi.org/10.1029/2008GB003327
Thompson, D.K., Woo, M.-K., 2009. Seasonal hydrochemistry of a high Arctic wetland complex. Hydrol. Process. 23, 1397–1407. https://doi.org/10.1002/hyp.7271
Trofimova, I.E., Balybina, A.S., 2014. Classification of climates and climatic regionalization of the West-Siberian plain. Geogr. Nat. Resour. 35, 114–122. https://doi.org/10.1134/S1875372814020024
Turetsky, M.R., Abbott, B.W., Jones, M.C., Anthony, K.W., Olefeldt, D., Schuur, E.A.G., Grosse, G., Kuhry, P., Hugelius, G., Koven, C., Lawrence, D.M., Gibson, C., Sannel, A.B.K., McGuire, A.D., 2020. Carbon release through abrupt permafrost thaw. Nat. Geosci. 13, 138–143. https://doi.org/10.1038/s41561-019-0526-0
Turunen, J., Tahvanainen, T., Tolonen, K., Pitkänen, A., 2001. Carbon accumulation in West Siberian Mires, Russia *Sphagnum* peatland distribution in North America and Eurasia during the past 21,000 years. Global Biogeochem. Cycles 15, 285–296. https://doi.org/10.1029/2000GB001312
van Huissteden, J., 2020. The Role of Ground Ice, in: van Huissteden, J. (Ed.), Thawing Permafrost. Springer, Cham, pp. 107–177. https://doi.org/10.1007/978-3-030-31379-1_3
Vasiliev, A.A., Drozdov, D.S., Gravis, A.G., Malkova, G. V, Nyland, K.E., Streletskiy, D.A., 2020a. Permafrost degradation in the Western Russian Arctic. Environ. Res. Lett. 15, 045001. https://doi.org/10.1088/1748-9326/ab6f12
Vasiliev, A.A., Gravis, A.G., Gubarkov, A.A., Drozdov, D.S., Korostelev, Y.V., Malkova, G.V., Oblogov, G.E., Ponomareva, O.E., Sadurtdinov, M.R., Streletskaya, I.D., Streletskiy, D.A., Ustinova, E.V., Shirokov, R.S., 2020b. Permafrost degradation: results of the long-term geocryological monitoring in the western sector of Russian Arctic. Earth`s Cryosphere XXIV, 14–26. DOI: 10.21782/KZ1560-7496-2020-2(15-30).
Vasiliev, A.A., Streletskaya, I.D., Shirokov, R.S., Oblogov, G.E., 2011. Evolution of cryolithozone of coastal zone of western Yamal during climate change. Kriosf. Zemli 2, 56–64.
Vasyukova, E. V., Pokrovsky, O.S., Viers, J., Oliva, P., Dupré, B., Martin, F., Candaudap, F., 2010. Trace elements in organic- and iron-rich surficial fluids of the boreal zone: Assessing colloidal forms via dialysis and ultrafiltration. Geochim. Cosmochim. Acta 74, 449–468.

https://doi.org/10.1016/j.gca.2009.10.026
Velichko, A.A., Timireva, S.N., Kremenetski, K.V., MacDonald, G.M., Smith, L.C., 2011. West Siberian Plain as a late glacial desert. Quat. Int. 237, 45–53. https://doi.org/10.1016/j.quaint.2011.01.013
Vonk, J.E., Mann, P.J., Davydov, S., Davydova, A., Spencer, R.G.M., Schade, J., Sobczak, W. V., Zimov, N., Zimov, S., Bulygina, E., Eglinton, T.I., Holmes, R.M., 2013. High biolability of ancient permafrost carbon upon thaw. Geophys. Res. Lett. 40, 2689–2693. https://doi.org/10.1002/grl.50348
Vonk, J.E., Tank, S.E., Bowden, W.B., Laurion, I., Vincent, W.F., Alekseychik, P., Amyot, M., Billet, M.F., Canário, J., Cory, R.M., Deshpande, B.N., Helbig, M., Jammet, M., Karlsson, J., Larouche, J., Macmillan, G., Rautio, M., Walter Anthony, K.M., Wickland, K.P., 2015. Reviews and syntheses: Effects of permafrost thaw on Arctic aquatic ecosystems. Biogeosciences. https://doi.org/10.5194/bg-12-7129-2015
Walvoord, M.A., Kurylyk, B.L., 2016. Hydrologic Impacts of Thawing Permafrost-A Review. Vadose Zo. J. 15, vzj2016.01.0010. https://doi.org/10.2136/vzj2016.01.0010
Wang, W., Wu, T., Zhao, L., Li, R., Xie, C., Qiao, Y., Zhang, H., Zhu, X., Yang, S., Qin, Y., Hao, J., 2018. Hydrochemical characteristics of ground ice in permafrost regions of the Qinghai-Tibet Plateau. Sci. Total Environ. 626, 366–376. https://doi.org/10.1016/j.scitotenv.2018.01.097
Weishaar, J.L., Aiken, G.R., Bergamaschi, B.A., Fram, M.S., Fujii, R., Mopper, K., 2003. Evaluation of specific ultraviolet absorbance as an indicator of the chemical composition and reactivity of dissolved organic carbon. Environ. Sci. Technol. 37, 4702–4708. https://doi.org/10.1021/es030360x
Yeghicheyan, D., Bossy, C., Bouhnik Le Coz, M., Douchet, C., Granier, G., Heimburger, A., Lacan, F., Lanzanova, A., Rousseau, T.C.C., Seidel, J.-L., Tharaud, M., Candaudap, F., Chmeleff, J., Cloquet, C., Delpoux, S., Labatut, M., Losno, R., Pradoux, C., Sivry, Y., Sonke, J.E., 2013. A Compilation of Silicon, Rare Earth Element and Twenty-One other Trace Element Concentrations in the Natural River Water Reference Material SLRS-5 (NRC-CNRC). Geostand. Geoanalytical Res. 37, 449–467. https://doi.org/10.1111/j.1751-908X.2013.00232.x
Zhang, T., Barry, R.G., Knowles, K., Heginbottom, J.A., Brown, J., 2008. Statistics and characteristics of permafrost and ground-ice distribution in the Northern Hemisphere. Polar Geogr. 31, 47–68. https://doi.org/10.1080/10889370802175895
Zong-Jie, L., Zong-Xing, L., Ling-Ling, S., Jin-Zhu, M., Yong, S., 2018. Environment significance and hydrochemical characteristics of supra-permafrost water in the source region of the Yangtze River. Sci. Total Environ. 644, 1141–1151. https://doi.org/10.1016/j.scitotenv.2018.07.029

805 **Table 1.** Physico-geographical and landscape characteristics of 5 study sites across the permafrost gradient in WSL.

806

Site	Lat., °N	Mean annual temp., °C	Mean annual precipit., mm	Mineral substrate	Micro-landscapes	Peat thickness, m	Seasonal thaw depth, cm	Soil type (WRB, 2014)
Tazovsky, (Tz)	67.4	–9.1	363	clay loam and loam	polygon	1.0–4.0	25–40	Dystric Hemic Epicryic Histosols (Hyperorganic); Dystric Murshic Hemic Epicryic Histosols (Hyperorganic)
					hollows	0.2–1.5	40–60	Dystric Fibric Cryic Histosols; Histic Reductaquic Cryosols (Clayic)
Nadym, (Nd)	65.3	–6.4	484	sand	peat mound	1.0–2.0	30–40	Epifibric Endohemic Cryic Histosols
	65.2			loam and sand	peat mound	0.2–1.0	40–50	Histic Cryosols, Epifibric Endohemic Cryic Histosols
Pangody, (Pg)	65.9	–6.8	490	loam	peat mounds	0.2–1.3	49	Dystric Hemic Epicryic Histosols; Histic Cryosols (Loamic); Histic Oxyaquic Turbic Cryosols (Loamic)
Khanymey, (Kh)	63.8	–5.6	540	sand	peat mounds	0.1–1.4	90	Dystric Hemic Cryic Histosols; Spodic Histic Turbic Cryosols (Albic, Arenic); Histic Turbic Cryosols (Albic, Arenic)

Table 2. Mean values with S.D. of dissolved (< 0.45 µm) elements in peat porewater (thawed, 0-30 cm) waters and peat ice (30-130 cm) in four sampled sites western Siberia Lowland. The DOC, DIC, Cl, SO_4^{2-}, Si, Ca, Mg, Na, K, P, Al and Fe concentrations are in mg/L with all other elements in µg/L.

Elements	Northern taiga (Khanymey) 63.79°N		Forest tundra (Pangody, Nadym) 65.87°N		Southern tundra (Tazovsky) 67.36°N		All WSL	
	thawed	frozen	thawed	frozen	thawed	frozen	thawed	frozen
DOC	74.2±26.7	472±305	102±49.8	266±312	61.2±15.7	585±563	82±39.1	426±418
DIC	4.42±2.58	4.97±3.41	3.5±1.28	8.42±5.54	4.64±1.09	9.11±8.89	4.11±1.8	7.54±6.41
Cl	2.47±1.77	1.37±1.5	1.30±0.93	0.73±0.46	1.49±1.53	0.75±0.53	1.76±1.48	0.93±0.94
$S\text{-}SO_4^{2-}$	0.54±0.31	1.62±1.66	0.4±0.11	0.16±0.14	0.29±0.21	2.9±3.3	0.34±0.3	1.72±2.52
Li	0.36±0.11	2.80±2.82	0.77±0.56	1.72±1.25	0.97±0.29	4.28±3.69	0.68±0.45	2.82±2.84
Be	0.011±0.006	0.04±0.02	0.04±0.04	0.06±0.04	0.03±0.01	0.07±0.03	0.03±0.03	0.06±0.03
B	150±259	54.4±43.9	84.1±126	60.6±47.1	54.5±26.7	47.6±21.0	98.2±169	54.8±39.8
Na	2.07±2.83	2.61±1.95	1.49±1.37	1.6±1.21	1.34±0.42	2.62±2.42	1.64±1.83	2.22±1.91
Mg	0.19±0.12	0.93±0.67	0.28±0.08	1.35±1.78	0.74±0.36	3.99±2.75	0.38±0.3	2.01±2.29
Al	0.21±0.11	1.18±0.89	0.33±0.16	0.54±0.46	0.44±0.18	0.85±0.48	0.32±0.17	0.83±0.67
Si	1.16±0.31	3.53±1.45	2.68±2.29	3.98±2.55	3.64±1.38	3.19±1.27	2.43±1.86	3.6±1.92
P	0.2±0.11	1.67±1.39	0.29±0.17	0.61±1.25	0.25±0.06	1.17±0.93	0.25±0.13	1.11±1.28
K	0.69±0.57	1.48±0.89	1.12±0.98	0.67±0.38	1.02±1.2	1.34±0.69	0.95±0.92	1.12±0.75
Ca	0.8±0.46	2.91±1.85	1.54±0.51	5.41±6.17	2.74±0.93	26.4±18.4	1.61±0.97	10.9±14.8
Ti	3.23±2.16	6.24±7.19	3.59±1.87	7.07±8.62	5.33±1.79	5.81±5.55	3.93±2.08	6.44±7.28
V	0.74±0.38	2.46±2.57	1.22±0.41	3.79±3.76	2.21±0.78	5.66±2.66	1.33±0.77	3.93±3.31
Cr	0.78±0.56	1.12±1.28	0.72±0.29	1.04±0.98	0.82±0.19	1.11±1.09	0.77±0.37	1.09±1.1
Mn	3.12±4.38	12.9±12.3	11.4±8.9	114±144	62.7±47.7	251±248	22.3±34.8	123±186
Fe	0.22±0.11	1.60±1.38	1.17±0.58	1.59±1.68	0.50±0.12	3.14±2.32	0.68±0.56	2.05±1.93
Co	0.17±0.06	1.00±0.68	1.67±0.80	1.99±1.88	1.06±0.27	5.77±3.54	1.01±0.83	2.81±3.01
Ni	0.68±0.32	3.79±2.57	2.5±1.1	3.88±2.22	2.58±0.69	11.15±5.46	1.91±1.18	6.02±4.88
Cu	1.3±1.45	1.14±0.7	0.77±0.33	2.42±3.27	1.67±0.48	2.49±1.41	1.19±0.94	2.04±2.27
Zn	178±237	535±393	215±433	83±89.4	82.4±29	463±455	167±303	338±390
Ga	0.07±0.05	0.17±0.14	0.05±0.03	0.1±0.08	0.08±0.04	0.13±0.12	0.07±0.04	0.13±0.12
Ge	0.006±0.004	0.01±0.02	0.01±0.00	0.02±0.02	0.02±0.01	0.02±0.01	0.01±0.007	0.02±0.02

As	0.85±0.52	2.07±1.9	0.97±0.56	10.6±18.8	0.88±0.35	6.04±3.99	0.91±0.48	6.57±12.4
Rb	0.87±0.53	6.52±3.66	3.01±3.09	2.83±1.68	1.7±0.72	12.8±10.1	1.94±2.17	6.97±7.17
Sr	7.06±3.83	27.1±15.5	13.2±5.7	37.7±40.4	15.3±2.98	133±91.9	11.7±5.55	62.8±72.5
Y	0.11±0.1	0.20±0.43	0.17±0.1	0.72±1.28	0.86±0.52	0.95±0.54	0.33±0.42	0.63±0.93
Zr	0.21±0.17	0.47±0.45	0.26±0.13	0.85±1.27	0.53±0.14	1.4±0.99	0.31±0.19	0.90±1.04
Nb	0.02±0.01	0.04±0.05	0.02±0.01	0.04±0.06	0.02±0.01	0.05±0.05	0.02±0.01	0.04±0.05
Mo	0.05±0.02	0.04±0.02	0.06±0.02	0.11±0.07	0.13±0.07	0.30±0.29	0.07±0.05	0.14±0.19
Cd	0.04±0.01	0.12±0.06	0.06±0.03	0.033±0.025	0.06±0.03	0.17±0.12	0.05±0.02	0.10±0.09
Sb	0.07±0.04	0.09±0.06	0.04±0.02	0.047±0.031	0.08±0.03	0.11±0.06	0.06±0.04	0.08±0.06
Cs	0.02±0.01	0.38±0.39	0.07±0.06	0.062±0.049	0.03±0.01	0.11±0.07	0.04±0.04	0.18±0.26
Ba	139±188	121±76	116±129	66±48	83.2±39.1	136±86	115±135	104±75.8
La	0.1±0.06	0.17±0.26	0.11±0.06	0.5±0.76	0.61±0.44	0.56±0.27	0.24±0.32	0.41±0.54
Ce	0.17±0.1	0.35±0.65	0.25±0.14	1.17±2.04	1.27±0.79	1.23±0.57	0.5±0.62	0.93±1.4
Pr	0.02±0.01	0.04±0.08	0.03±0.02	0.15±0.26	0.15±0.09	0.16±0.08	0.06±0.07	0.12±0.18
Nd	0.07±0.05	0.16±0.33	0.12±0.07	0.63±1.14	0.64±0.35	0.69±0.33	0.24±0.3	0.5±0.78
Sm	0.02±0.01	0.04±0.07	0.06±0.04	0.17±0.26	0.15±0.08	0.16±0.08	0.07±0.07	0.13±0.18
Eu	0.02±0.02	0.02±0.02	0.015±0.01	0.04±0.06	0.04±0.02	0.05±0.02	0.02±0.02	0.03±0.04
Gd	0.02±0.02	0.04±0.08	0.03±0.02	0.15±0.26	0.17±0.09	0.17±0.08	0.07±0.08	0.12±0.18
Tb	0.003±0.003	0.01±0.01	0.005±0.003	0.02±0.03	0.03±0.01	0.02±0.01	0.01±0.01	0.02±0.02
Dy	0.021±0.02	0.03±0.06	0.03±0.02	0.12±0.21	0.14±0.08	0.15±0.07	0.06±0.07	0.1±0.15
Ho	0.004±0.004	0.01±0.01	0.007±0.004	0.02±0.05	0.03±0.01	0.03±0.01	0.01±0.01	0.02±0.03
Er	0.01±0.01	0.02±0.04	0.02±0.01	0.07±0.14	0.08±0.04	0.10±0.05	0.03±0.04	0.06±0.1
Tm	0.0015±0.001	0.003±0.006	0.003±0.002	0.01±0.02	0.01±0.005	0.01±0.008	0.00±0.00	0.01±0.01
Yb	0.0083±0.007	0.02±0.04	0.02±0.01	0.08±0.14	0.07±0.03	0.10±0.06	0.03±0.03	0.07±0.10
Lu	0.0013±0.001	0.003±0.006	0.003±0.002	0.01±0.02	0.01±0.004	0.02±0.01	0.004±0.005	0.01±0.02
Hf	0.008±0.007	0.02±0.02	0.01±0.005	0.03±0.05	0.02±0.01	0.06±0.05	0.01±0.008	0.04±0.04
W	0.06±0.04	0.05±0.06	0.02±0.02	0.08±0.11	0.03±0.01	0.03±0.03	0.04±0.03	0.06±0.08
Tl	0.007±0.005	0.03±0.02	0.02±0.01	0.01±0.01	0.01±0.004	0.02±0.008	0.01±0.01	0.02±0.01
Pb	0.47±0.39	0.53±0.38	0.39±0.23	0.20±0.14	0.39±0.22	0.47±0.36	0.41±0.28	0.39±0.33
Th	0.03±0.02	0.06±0.13	0.06±0.05	0.08±0.11	0.18±0.15	0.08±0.04	0.08±0.10	0.08±0.10
U	0.01±0.006	0.02±0.02	0.007±0.005	0.02±0.04	0.06±0.05	0.15±0.14	0.02±0.03	0.06±0.10

Table 3. Mean ±SD depth integrated surface-normalized pools of dissolved (< 0.45 µm) elements in 0-30 cm (active layer) and 30-130 cm (frozen layer).

Elements		Northern taiga (Khanymey) 63.785°N		Forest tundra (Pangody, Nadym) 65.873°N		Southern tundra (Tazovsky) 67.357°N	
		0-30 cm	30-130 cm	0-30 cm	30-130 cm	0-30 cm	30-130 cm
DOC	g m²	13.1±0.19	348±271	25.4±24.8	207±69	10.4±2.91	544±455
Cl^-	mg m²	628±265	850±350	120±48	758±161	171±11.3	821±275
S-SO_4^{2-}	mg m²	124±4.4	1105±238	31±8.3	104±15	60±40	2668±3033
Li	mg m²	0.08±0.01	1.81±0.43	0.25±0.27	1.31±0.53	0.16±0.05	4.03±3.69
Be	µg m²	1.35±0.18	40.2±6.12	13±15.5	45.9±25.3	6.82±2.64	69.1±35
B	mg m²	20.8±28.4	35.3±40.2	12.6±12.2	73.4±88.2	10.2±0.73	45.3±5.49
Na	g m²	0.32±0.3	1.74±0.78	0.26±0.02	1.21±0.45	0.22±0.03	2.04±0.62
Mg	g m²	0.03±0.01	0.68±0.63	0.06±0.04	0.82±0.33	0.11±0.06	3.62±1.56
Al	g m²	0.03±0.01	0.7±0.62	0.09±0.09	0.35±0.06	0.09±0.04	0.8±0.48
Si	g m²	0.25±0.06	3.09±0.3	0.36±0.21	2.64±0.66	0.6±0.27	3.14±0.56
P	g m²	0.05±0.01	1.51±0.25	0.06±0.05	0.5±0.14	0.05±0.01	1.07±0.73
K	g m²	0.17±0.04	1.22±0.1	0.24±0.23	0.63±0.49	0.11±0.01	1.34±0.08
Ca	g m²	0.09±0.06	2.15±2.11	0.3±0.17	3.47±0.29	0.44±0.12	24.2±16.3
Ti	mg m²	0.52±0.21	3.05±0.81	0.93±0.54	3.37±1.31	1.06±0.19	5.49±1.61
V	mg m²	0.17±0.02	2.54±1.16	0.29±0.22	2.16±1.13	0.41±0.11	5.16±2.31
Cr	mg m²	0.18±0.02	0.72±0.11	0.16±0.1	0.59±0.11	0.16±0.003	1.03±0.51
Mn	mg m²	0.71±0.7	10.3±11	1.63±0.92	69.1±9	9.99±11.1	238±238
Fe	g m²	0.04±0.004	1.28±1.28	0.25±0.15	0.92±0.1	0.09±0.01	2.81±0.2
Co	mg m²	0.03±0.005	0.93±0.62	0.36±0.37	1.46±0.66	0.18±0.06	5.29±2.74
Ni	mg m²	0.16±0.02	3.99±1.8	0.5±0.39	2.94±0.44	0.42±0.07	10.2±5.08
Cu	mg m²	0.25±0.1	0.91±0.12	0.16±0.004	1.76±1.89	0.33±0.07	2.23±0.54
Zn	mg m²	24.9±29.3	330±326	17±17.3	168±228	15.2±2.58	474±581
Ga	µg m2	9.7±5.36	98.2±76.4	15.9±14.6	55.8±0.78	16.4±4.39	120±63.6
Ge	µg m²	1.3±0.23	7.43±1.21	2.38±1.53	12.7±1.92	3.17±0.75	14.2±5.39
As	mg m²	0.15±0.05	2.29±0.32	0.12±0.03	5.77±5.19	0.17±0.04	5.16±3.38
Rb	µg m2	0.25±0.13	6.14±0.24	712±900	2523±1733	240±68.5	11808±1284
Sr	mg m²	0.98±0.43	20.8±15.4	2.76±2.05	24.1±3.6	2.61±0.1	122±83.1

Y	µg m²	17.6±3.63	296±287	32.3±15.7	231±212	183±129	862±387
Zr	µg m²	35.7±16	344±39.3	43.7±9.80	312±122	102±13.1	1273±616
Nb	µg m²	2.85±0.87	15.7±2.18	4.85±3.9	18.1±4.15	4.75±0.88	48.9±29
Mo	µg m²	10.1±1.99	36.5±11.7	14.3±11.5	105±80	26±8.89	262±192
Cd	µg m²	5.99±0.05	93.2±69.7	12±11	29±4.4	10.3±4.81	166±121
Sn	µg m²	104±134	188±83.2	6.42±2.74	11.2±1.32	4.15±1.1	41.1±22.9
Sb	µg m²	13.1±0.79	91.7±44.3	8.12±0.64	40±37.8	16.5±1.01	105±61.5
Cs	µg m²	5.97±4.35	287±3.95	18.1±22.8	45.7±14	4.5±0.16	97.8±18.2
Ba	µg m²	18.9±24.6	102±32.5	14.4±13.8	69.3±65	15.4±2.37	132±89.5
La	µg m²	16.7±2.99	201±173	26.1±20.8	210±147	136±114	502±40.9
Ce	µg m²	27.3±1.43	463±435	59.7±49.3	400±302	278±205	1100±184
Pr	µg m²	3.01±0.06	53.2±50	6.82±5.5	50.4±44.9	33.3±23.1	143±38.5
Nd	µg m²	11.6±0.09	229±222	27.3±21.2	210±195	139±90.8	631±198
Sm	µg m²	3.91±0.31	57.5±51.6	8.14±3.72	78.7±86.8	33.1±19.9	143±46
Eu	µg m²	2.3±2.11	19.7±8.11	2.48±0.48	15.9±14.7	9.05±5.19	43.8±17.7
Gd	µg m²	3.43±0.69	56.7±54.2	6.9±4.4	50.5±45.9	36.5±22.9	152±46.5
Tb	µg m²	0.51±0.1	7.55±7.33	1.06±0.62	7.24±6.87	5.36±3.67	21.7±6.67
Dy	µg m²	3.29±0.86	45.4±43.3	6.87±3.37	41.2±39.1	30.2±19.8	134±45.3
Ho	µg m²	0.6±0.24	9.54±8.87	1.25±0.53	7.95±7.44	5.71±3.5	27.5±9.71
Er	µg m²	1.59±0.46	28.2±26.9	3.3±1.48	22.4±20.6	16.9±9.92	87.9±37.2
Tm	µg m²	0.22±0.09	4.36±3.38	0.46±0.17	3.21±3.03	2.28±1.12	13.2±6.01
Yb	µg m²	1.28±0.68	26.1±23.6	2.88±0.68	22.4±21	14.4±6.53	92.2±42.7
Lu	µg m²	0.23±0.13	4.38±3.65	0.44±0.13	3.62±3.6	2.19±0.88	15±7.85
Hf	µg m²	1.22±0.52	13.3±0.21	1.62±0.58	11.8±3.09	3.8±0.44	49.9±26.6
W	µg m²	8.66±0.72	43.1±47	3.06±0.28	37.9±35.1	4.52±1.23	26.5±1.81
Tl	µg m²	1.11±0.07	24.1±1.64	1.5±1.08	11±4.93	1.58±0.3	17.7±9.85
Pb	µg m²	75.9±38.5	380±359	87.6±36.7	161±121	77.7±11.5	469±419
Th	µg m²	3.75±0.22	25.8±2.6	14.1±15.5	39±7.8	41.6±37.3	73.3±7.55

Table 4. Comparison of annual dissolved (< 0.45 μm) element delivery due to 100-cm thawing of peat ice (assuming the rate of ALT increase of 1 cm y^{-1} over the next 100 years) to the current riverine elementary yield (kg/km²/y) in the permafrost. The sites of peat core sampling in this study are located within the river watersheds analyzed by Pokrovsky et al. (2020). Note that the watersheds of permafrost-affected WSL rivers are essentially presented by frozen peat bogs (Krickov et al., 2019).
* stands for data of Pokrovsky et al. (2020).

Element	Thawing of peat ice	Current riverine yield*	% of riverine increase due to peat thaw
Zn	3.24±3.78	1.42±0.89	228
P	10.3±3.7	5.71±2.3	180
Cs	0.001±0.0001	0.001±0.0005	143
C_{org}	3664±2649	3399±1279	108
Co	0.03±0.01	0.07±0.04	39
Ba	1.01±0.62	2.95±1.4	34
Cd	0.001±0.001	0.003±0.001	32
As	0.04±0.03	0.14±0.047	31
Al	6.13±3.88	20.4±11	30
Rb	0.05±0.01	0.16±0.059	30
Ga	0.001±0.0005	0.004±0.002	23
Mo	0.001±0.001	0.006±0.002	22
Fe	16.7±5.28	92.2±42	18
Ni	0.06±0.02	0.32±0.15	18
SO_4	38.7±32.9	234±116	17
U	0.0005±0.0002	0.003±0.001	16
Pb	0.003±0.003	0.02±0.01	14
Nb	0.0003±0.0001	0.002±0.001	14
B	0.51±0.45	3.82±1.8	13
Ca	99.5±62.3	1004±368	9.9
K	10.6±2.24	108±36	9.9
Cu	0.02±0.01	0.18±0.087	9.2
Th	0.0005±0.0001	0.005±0.003	9.2
Sb	0.0008±0.0005	0.009±0.004	8.8
Y	0.005±0.003	0.06±0.03	8.3
Yb	0.0005±0.0003	0.006±0.003	7.8
Dy	0.0007±0.0004	0.01±0.006	7.4
Nd	0.004±0.002	0.05±0.03	7.3
Ce	0.007±0.003	0.09±0.051	7.2
Pr	0.0008±0.0004	0.01±0.007	6.9
Mn	1.06±0.86	16.9±11	6.3
Sr	0.56±0.34	9.12±4.8	6.1
La	0.003±0.001	0.05±0.026	6.1
Li	0.02±0.02	0.45±0.18	5.2
Hf	0.0002±0.0001	0.005±0.003	5.0
Mg	17±8.4	414±125	4.1
Cr	0.008±0.002	0.2±0.08	3.8
Ti	0.04±0.01	1.4±0.52	2.8
Si	29.6±5.08	1076±430	2.7
Na	16.6±6.18	1116±592	1.5
Cl	8.1±2.62	1150±692	0.7
Zr	0.006±0.003	1.57±0.6	0.4

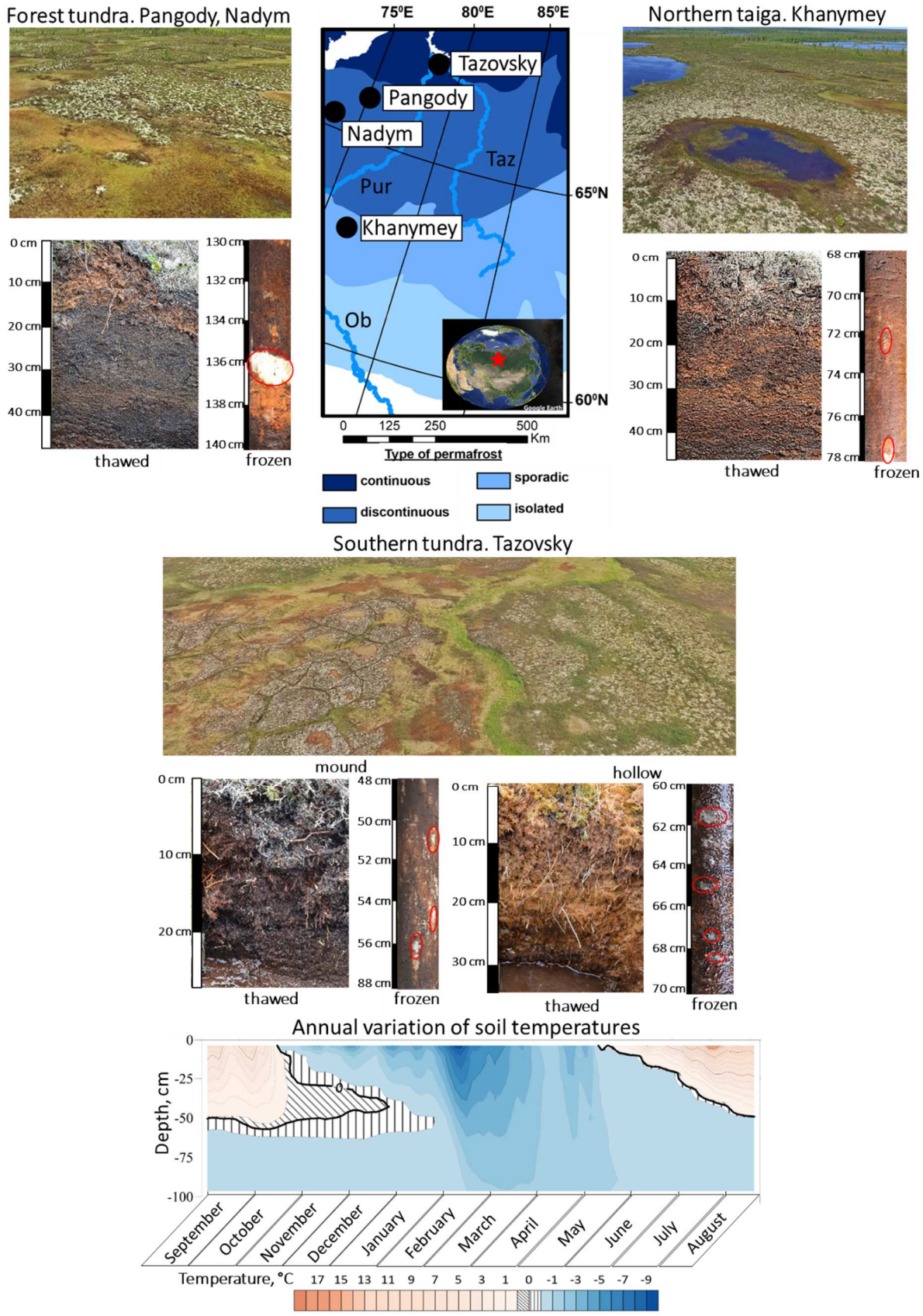

Figure 1. Study sites and illustration of active layer and sampled peat cores. Map of the study site including permafrost boundaries (Brown et al., 2002; http://portal.inter-map.com (NSIDC)) and the 4 test sites – Khanymey, Pangody, Nadym and Tazovsky. The bottom diagram represents annual

variation in soil temperatures for the Khanymey site: direct measurements of soil temperature by loggers (IMKES SB RAS, Russia) since their installation on 27 August 2018 till 17 August 2019.

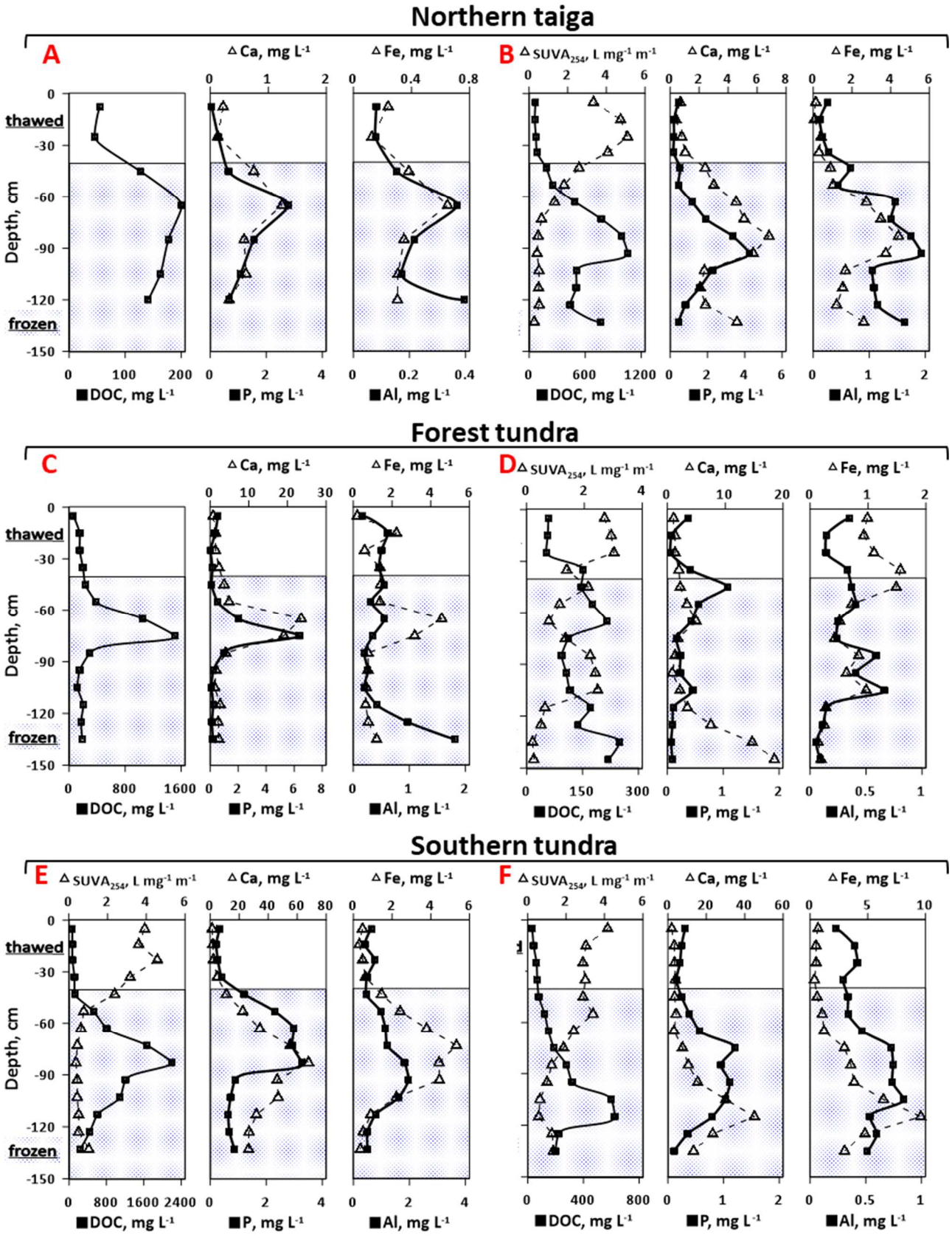

Fig. 2. The measured profiles of dissolved (< 0.45 μm) DOC, SUVA, P, Ca, Al, Fe, Na and Cl in sampled peat cores (porewater of active layer and permafrost ice) in northern taiga (Khanymey) (**A, B)**, forest tundra (Pangody, Nadym) (**C**, **D)** and southern tundra (Tazovsky) (**E, F).**

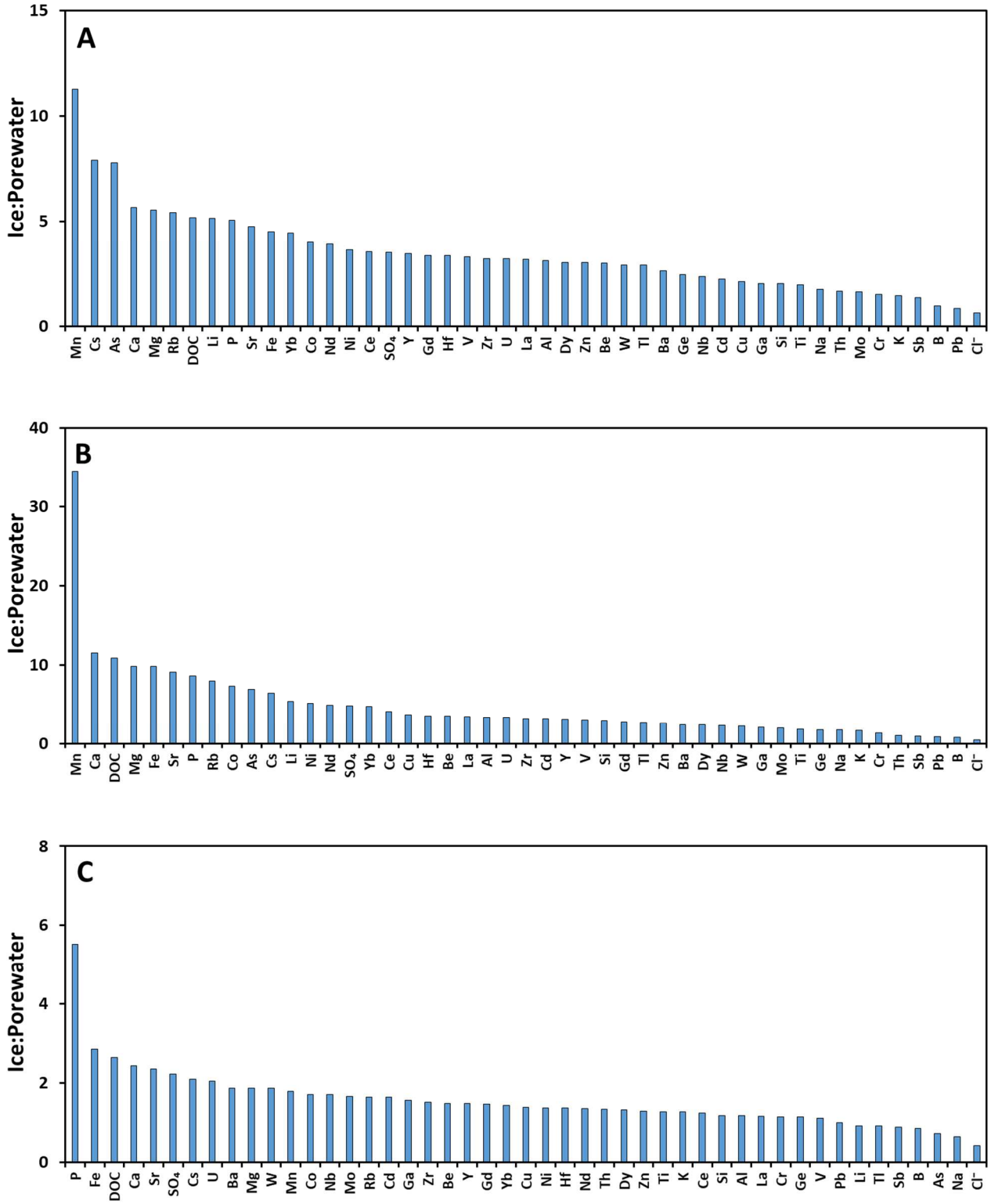

Figure 3. The ratio of dissolved (< 0.45 μm) elemental concentrations in peat ice compared to peat porewaters collected from positive forms of micro-relief (mound, polygon) **(A);** the ratio of maximal concentration at the peak to the average value of the two most surface layers (0-10 and 10-20 cm depth) **(B)** and to the two most deep (130-120 cm and 120-110 cm) layers **(C)** across all the permafrost zones. To draw these plots we used mean WSL values from Table 2.

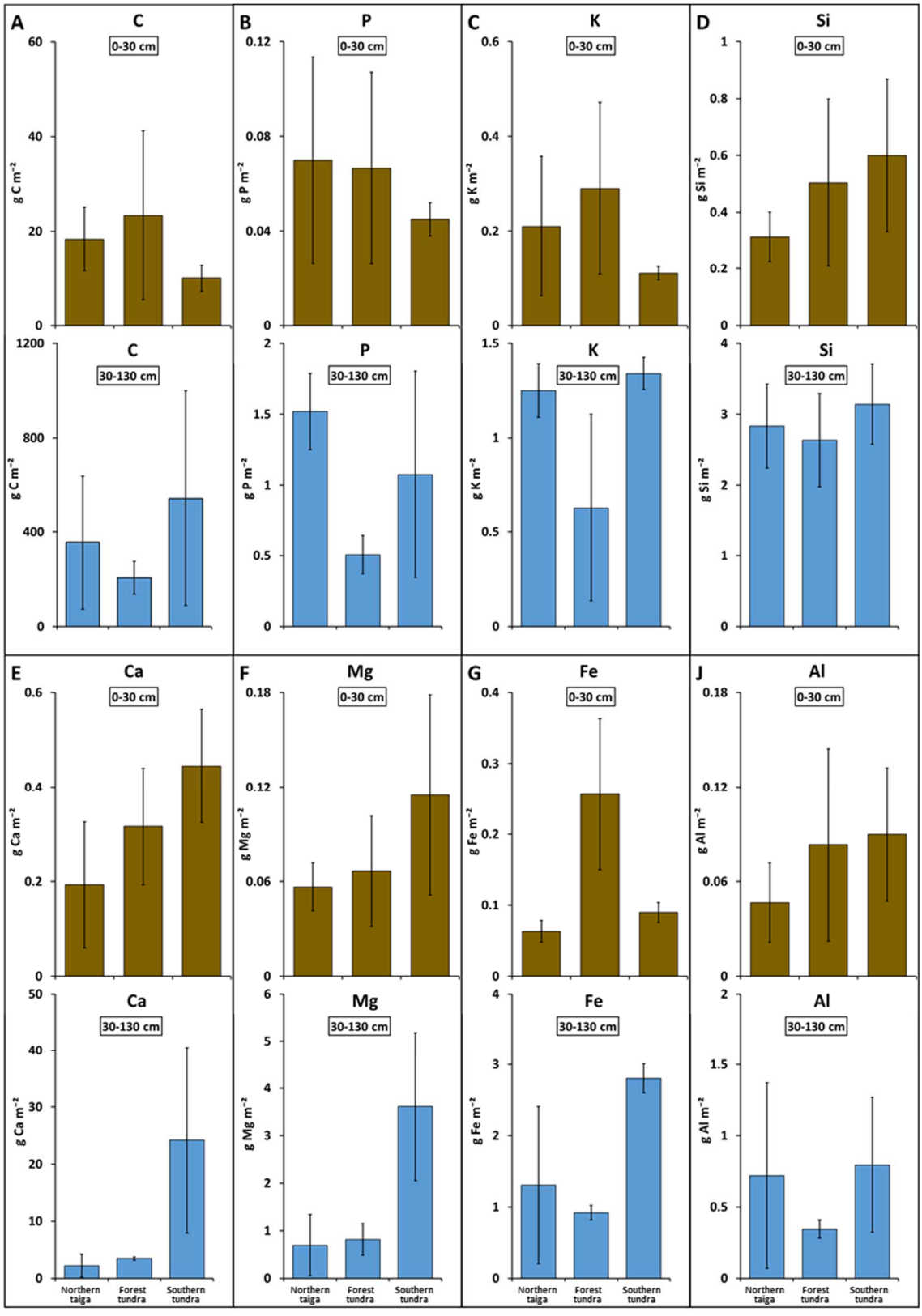

Figure 4. Depth-integrated, surface-normalized pools of dissolved (< 0.45 μm) DOC **(A)**, P **(B)**, K **(C)**, Si **(D)**, Ca **(E)**, Mg **(F)**, Fe **(G)** and Al **(J)** in peat porewater of the active layer (0-30 cm) and the permafrost ice (30-130 cm) in various permafrost zones of western Siberia. The northern taiga (Khanymey), forest tundra (Pangody, Nadym) and soujern tundra (Tazovsly) correspond to sporadic, discontinuous and continuous permafrost zones, respectively.

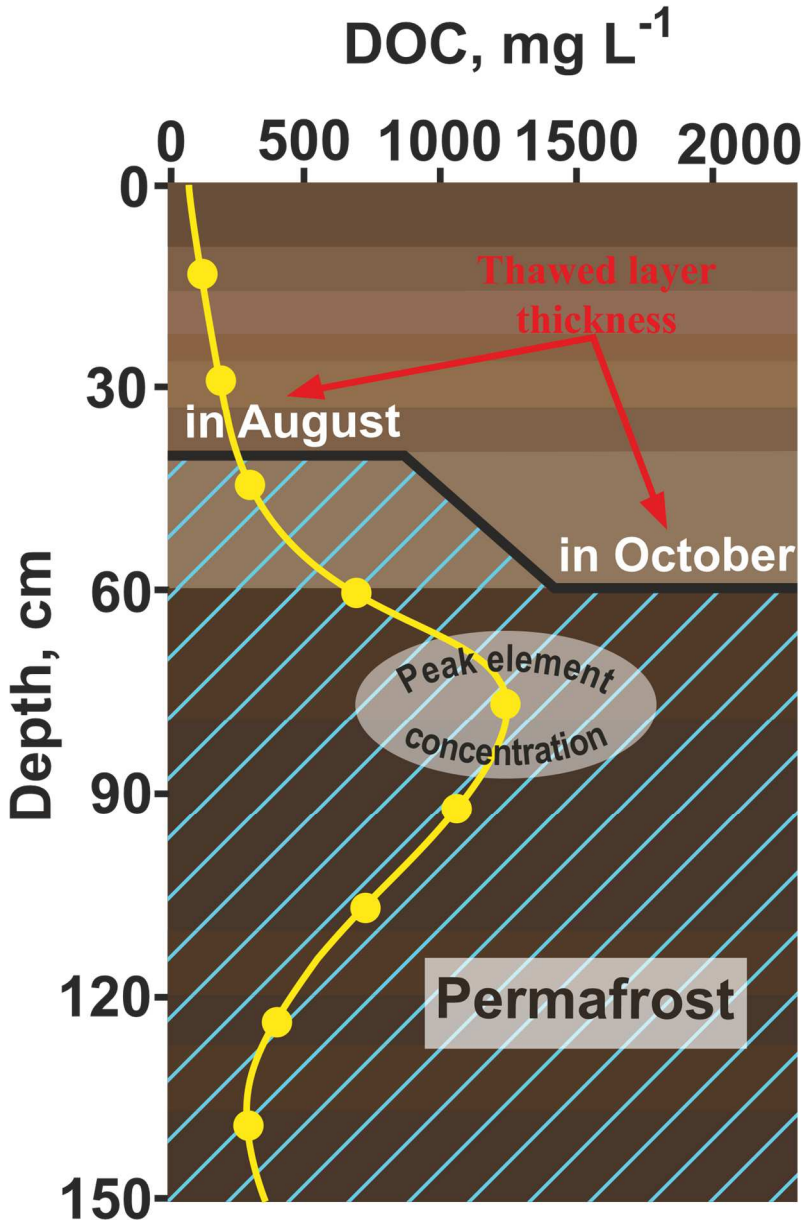
DOC, mg L-1
0
500
1000
1500
2000
0
30
60
90
120
150
Depth, cm
Thawed layer thickness
in August
in October
Peak element concentration
Permafrost